The Origins and Use of Various Code Specifications and Design Guides for Concrete Slabs-on-Ground in Hangar Applications

by

Ciara N. Morgan

A thesis submitted to the Graduate Faculty of
Auburn University
in partial fulfillment of the
requirements for the Degree of
Master of Science

Auburn, Alabama
May 4, 2019

Keywords: Slabs-on-ground, hangar foundations, Westergaard, slab thickness, design method origins, factors of safety

Approved by

James S. Davidson, Gottlieb Endowed Professor of Civil Engineering
Robert W. Barnes, Associate Professor of Civil Engineering
Mary L. Hughes, Lecturer, Assistant Chair of Undergraduate Studies, Civil Engineering
Alessandra Bianchini, Airbase Recovery and Acquisition Subject Matter Expert, Air Force Civil Engineer Center

ABSTRACT

Research focused on the origins and applications of various code specifications and design guides used in the design of concrete slabs-on-ground in airplane hangar foundations. This thesis investigates the mathematical origins and theories used in the creation of design charts and nomographs from the American Concrete Institute, the Portland Cement Association, the Unified Facilities Criteria, and the Corps of Engineers. Consideration was also given to the use of built-in safety provisions such as load factors as well as designer-selected safety provisions in the design of slabs-on-ground. This thesis also describes the ideal approach to designing and analyzing slabs-on-ground in the application of hangar foundations.

Results revealed that the best approach to designing and analyzing slabs-on-ground is dependent on the loading conditions and application of the slab. It was determined that the American Concrete Institute's Committee 360 guide to design of slabs-on-ground is based on a number of different methods including the direct application of equations derived by Harold M. Westergaard, a pioneer in the field of plates on elastic foundations, as well as the use of the Portland Cement Association and Corps of Engineers methods for slab thickness selection. Furthermore, it was determined that the United States Department of Defense's Unified Facilities Criteria method for slab thickness selection is based on the Corps of Engineers method, which is partially based on Westergaard's equations for loads placed at the edge of slabs-on-ground. In addition, this research determined that the Portland Cement Association method for determining

slab thickness is based on Westergaard's equations for loads placed at the interior of slabs-on-ground.

After determining the origins of the various code specifications and design guides, research was conducted to determine if any factors of safety are built into the design charts and nomographs within the codes and guides for selecting slab thickness. It was determined that there is no factor of safety built into the design chart used in the Portland Cement Association method, but that there is a factor of safety built into the design chart used in the Unified Facilities Criteria and Corps of Engineers methods.

ACKNOWLEDGEMENTS

I am grateful to my advisor, Dr. Davidson, for providing insight along the way and for my defense committee members Drs. Barnes and Hughes for taking the time to listen to and give input on my defense. Thank you to my sponsors, Dr. Dinan and Mr. Deel, at the Tyndall Air Force Civil Engineer Center (AFCEC), for providing me this academic opportunity. I also want to recognize Dr. Bianchini at AFCEC for her helpful input throughout my research. I am grateful to the Oak Ridge Institute for Science and Education for their monetary support for this endeavor. I would also like to thank my loved ones for their support and encouragement throughout the process.

TABLE OF CONTENTS

LIST OF FIGURES

LIST OF TABLES

CHAPTER 1: INTRODUCTION

1.1 BACKGROUND

To understand the issues with current code specifications and design guides used for the design of concrete slabs-on-ground, the definition of "slab-on-ground" and its behavior are first introduced. A slab-on-ground is defined as a concrete slab whose primary purpose is to support the given loads applied to it by bearing on the ground that it rests on and is supported by (ACI 360R-10). In the application of hangar foundations, we are usually concerned with slabs that are acting as rigid pavements due to the fact that hangar floors not only carry dead loads and live loads such as people, furnishings, and mechanical equipment, but also vehicle loads in the form of aircraft and servicing vehicles such as re-fuelers and mechanics' trucks. Rigid pavements support wheel loads via flexural resistance, in contrast to flexible pavements such as those consisting of multiple unbonded layers usually topped with a thin layer of asphalt (Ioannides et al., 1985), which dissipate loads to the subgrade over multiple layers of increasing areas. There are two main categories of slabs-on-ground, reinforced and unreinforced, which are both comprised of the following basic parts: the slab itself and the joints as explained in the following paragraph. Pavement slabs are often unreinforced whereas structural slabs are reinforced, although it is common for rigid pavements to include some reinforcement intended to prevent cracking by allowing for physical phenomenon such as restrained shrinkage and expansion, among others.

Reinforced and unreinforced concrete slabs-on-ground consist of several smaller slab segments connected by joints. Placing a concrete slab-on-ground without joints would result in many problems including severe cracking, which is why the slab is essentially broken up into segments connected by joints to make up the entirety of the slab-on-ground. Whether the slab-on-ground is reinforced or not is up to the design engineer depending on the loading scenario, the preferred design approach, and code specification requirements.

In the design of concrete slabs-on-ground, engineers rely on their knowledge of slabs-on-ground from education and experience as well as code specifications and design guides meant to assist in designing a slab that performs well in the given scenario. There are many code specifications and design guides written by various organizations such as the Portland Cement Association (PCA), the American Society of Civil Engineers (ASCE), the American Concrete Institute (ACI), and for the military, the Unified Facilities Criteria (UFC), and the Corps of Engineers (COE). These codes and guides sometimes contain built-in provisions or factors of safety used to account for potential errors in design calculations and construction and variability of the loads, material properties, and support conditions. Other times, the factor of safety is up to the designer to select and employ.

Sometimes, it is difficult to easily recognize the presence of built-in provisions, especially in design aides in the form of charts or nomographs and it is difficult to trace the mathematical origins that were used in the creation of the design charts and nomographs. If it is not clear to a designer that there is a factor of safety already included within an equation, chart, or graph, the resulting structure could be inefficiently designed, which would result in unnecessary use of materials and money wasted.

In the case of visual aids such as design charts and nomographs, the designer starts with a known value or values and uses the tool to determine results for an unknown value. The lines and curves in such tools are based on extensive research conducted and compiled into an "easy-to-use" design guide. In fact, these design aids are intended to *guide* the designer in the computations involved in designing a slab-on-ground, and they should not be used without understanding the mechanical principles applied to develop them. The design aids specific to this thesis are based on ideas from the early 1800s and have evolved over the last 200+ years. The original mathematical computations conducted by engineers such as Emil Winkler and Harold M. Westergaard, among others, are difficult to trace or sometimes incorrect.

With the introduction of computerized methods of structural analysis, it is less common to study the arduous calculus required to design and analyze slabs-on-ground by hand. With that comes the opportunity to misinterpret input and output values and misapplication of design tools, which is discussed further in this thesis in later chapters. Furthermore, historical provisions and factors of safety may not be consistent with current design philosophy, material properties, or construction properties. For these reasons, it is worth investigating the origins and applicability of the various code specifications and design guides for slabs-on-ground.

1.2 OBJECTIVE(S)

The objective of this research was to determine the origins of the design charts and nomographs used for the selection of slab-on-ground thickness from ACI, PCA, UFC, and COE. In addition, this research identified current built-in factors of safety, if any, included in the afore-mentioned code specifications and design guides and to determine if these factors of safety are still relevant to current state-of-the-art design processes. Finally, this research described the

differences between the various design ideologies and determine which one, if any, is best for use in the design and analysis of slabs-on-ground in the application of hangars.

1.3 SCOPE OF METHODOLOGY

Following a thorough investigation into the origins of the design charts and nomographs, this research attempted to establish a logical explanation for the accurate use of these design aids, backed by mathematical and mechanical evidence. This investigation occurred in the form of an extensive historical review of the computational evolution of the design and analysis of slabs-on-ground. Calculations were conducted to establish a connection between the design charts and nomographs and the mathematical theories and laws that these charts are supposedly based on according to the citations within each design guide and code specification. Further calculations were attempted to identify built-in factors of safety in the current code specifications and design guides.

This investigation did not address temperature and curling effects, moisture sensitivity, and fracture mechanics of concrete slabs-on-ground. Though these elements are important to the design and analysis of slabs-on-ground and mentioned briefly in the literature review in Chapter 2, focus was placed on the selection of slab-on-ground thickness methods.

1.4 THESIS ORGANIZATION

Organized into chapters, the following thesis includes Chapter 2, a comprehensive literature review of pertinent material relating to the behavior, design, analysis, and failure modes of slabs-on-ground in addition to the past research and current design methodologies. The literature reviewed includes current code specifications and their predecessor documents, current design guides and their respective predecessors, other research conducted and published related to this topic, and journal articles meant to add clarification to current code specifications or

design methods. Chapters 3 and 4 present an expansion on this material. Chapter 3 is an in-depth historical review of the origins of the mathematical and theoretical approaches to the design and analysis of slabs-on-ground. Chapter 4 contains calculation set-up and a description of computation methods used as well as computations and results from these calculations and a discussion of results. Chapter 5 provides a conclusion on the findings as well as suggestions for future work.

CHAPTER 2: LITERATURE REVIEW

2.1 OVERVIEW

This literature review aims to describe current knowledge on the design and analysis of slabs-on-ground, their failure modes and behavior, and current code provisions and design guides.

2.2 BEHAVIOR, DESIGN, AND ANALYSIS OF SLABS-ON-GROUND

There exist four basic types of slabs: unreinforced slabs-on-ground, slabs-on-ground with reinforcement to limit cracking, slabs-on-ground with reinforcement to prevent cracking, and structural slabs (ACI 360R-10). Structural slabs are not relevant in the case of this research since they are not in contact with the ground and are therefore governed by ACI 318-14: Building Code Requirements for Structural Concrete. It is important to note that "slab-on-ground" and "slab-on-grade" are used synonymously throughout literature reviewed to refer to a slab that is in contact with the soil as opposed to a structural floor slab but are referred to as a "slab-on-ground" for the purpose of this report. The term "grade" defines the soil that has been prepared for construction by earth removal and fill, and compaction. It is a construction term, so the term "ground" better fits the theoretical application of design and analysis. The first three slab types mentioned above, excluding structural slabs governed by ACI 318, are discussed in this research thesis. More specifically, this research encompassed the design and analysis of these slab-on-ground types in hangar foundation applications. After understanding the types of

slabs-on-ground that exist, it is important to understand how they behave and how they are designed and analyzed.

Slabs-on-ground are idealized for design and analysis purposes as Westergaard plates resting either on a Winkler subgrade, that is, having dense liquid behavior (Winkler, 1868), or on a Boussinesq subgrade, elastically solid in behavior (Boussinesq, 1885). For this reason, "slab-on-ground" is used interchangeably with "plate" throughout this research paper. Special consideration was given to dense liquid subgrade behavior in the application of this research since it was the most frequently used subgrade behavior idealization in the works of Westergaard, an engineer central to the development of slab-on-ground design and analysis.

Fundamental research conducted by Harold M. Westergaard and Emil Winkler, which was expanded upon by many others as discussed in Chapter 3, resulted in a classical approach to designing and analyzing slabs-on-ground that is still used today. Westergaard theorized the behavior of a slab-on-ground as a plate that rests on a subgrade, which reacts at infinitely many points as linear springs, each independent of the other (Ioannides, 1984). The springs have a proportionality constant *k*, called a modulus of subgrade reaction, as shown in Figure 2-1. The theoretical slab was considered homogeneous, isotropic, and behaving elastically. Figure 2-1 shows the slab simply supported along its edges and having a modulus of elasticity, *E*, Poisson's ratio, *v*, thickness, *h*, loaded by a uniformly distributed load, *w*, and resting on a Winkler subgrade with a modulus of subgrade, *k*.

The modulus of subgrade is based on the idea that the ratio of contact pressure to deflection, δ, is the same at every point of the slab (Winkler, 1868) as demonstrated in Equation 2-1 (Ioannides et al., 1985). The properties of the soil where the slab is placed define the modulus of subgrade reaction. According to research conducted by Dey et al. (2011), the

modulus of subgrade reaction is dependent on the loading conditions because of its effects on the confining pressure existing in the subgrade. Winkler called this idealization of subgrade a "dense liquid". A dense liquid subgrade is best thought of as behaving similarly to an elastic rubber foundation (Brink, 2003). Brink used rubber mats to simulate a liquid Winkler foundation with or without sublayers. Chapter 3 of this thesis provides a more extensive timeline of the developments that have been made in slab-on-ground design and analysis since the original works of Westergaard.

$$\sigma(x, y) = k\delta(x, y) \tag{2-1}$$

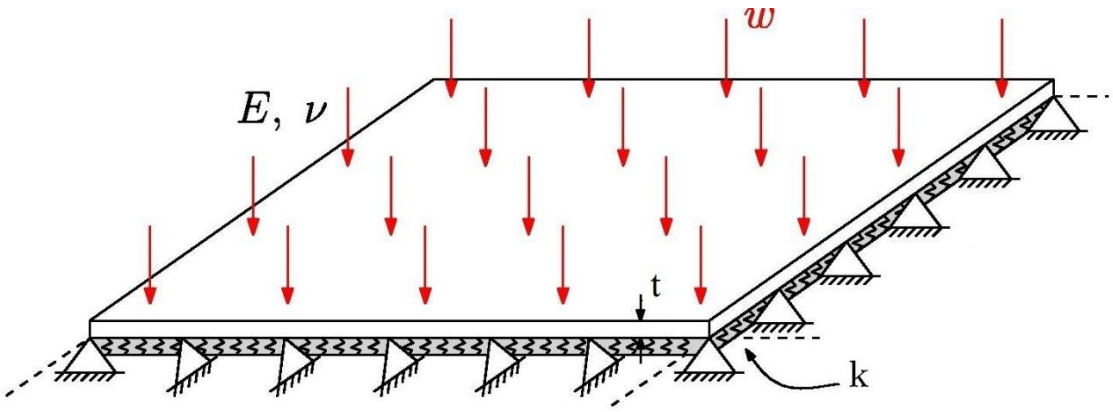

Figure 2-1: A Slab Resting on a Winkler Subgrade with Continuous Edge Supports and Distributed Load, *w* (Valdebenito et al., 2016)

2.3 FAILURE MODES OF SLABS-ON-GROUND

Having a better understanding of the design basis cited by current code specifications and design guides and how to use them can help us better understand how to prevent failures. In the application of hangar foundations, tolerances for cracking in slabs-on-ground are extremely low due to the potential for Foreign Object Damage (FOD) to the aircraft and equipment stored in hangars. Defined in the Whole Building Design Guide (WBDG), FOD hazards are created when

debris made up of bits of concrete resulting from cracking of the slab causes damage to something being stored in the hangar such as the jet propulsion mechanisms of a stored aircraft (Donnally, 2016). Many code specifications and design methods are aimed at either minimizing or eliminating altogether these types of slab failure. For the purpose of limiting or preventing cracks, slabs can be designed as either unreinforced or reinforced.

In addition to reinforcement methods, joints are used to improve slab performance, specifically to prevent cracking, through strategic placement. Joints have three general uses and can be divided into three types: contraction joints, construction joints, and isolation joints. Contraction joints are included in the design of a slab-on-ground to allow for the expansion and contraction of the concrete slabs that occurs naturally with changes in temperature and moisture and cement hydration reactions. Without this allowance for expansion and contraction, damage could occur that may be not only detrimental to the performance of the concrete slab, but is also aesthetically displeasing. Construction and isolation joints are also useful in the construction process by breaking up the segments placed at different intervals and by isolating some slab segments from others that may serve different purposes or handle different loading patterns such as near wall or column loads (UFC 3-320-06A). Joints in slabs-on-ground, while necessary, affect the overall response of the slab to loads. The slab stresses vary depending on proximity of the load to a joint. This point is further discussed in Section 3.2.3.

2.4 CURRENT CODE PROVISIONS AND DESIGN CHARTS AND NOMOGRAPHS

There exist several codes and design guides related to the design of concrete slabs-on-ground. Different committees and organizations formed each one, which can be a problem when each one may have been not only based on different design theories or methodologies, but may also vary just based on the opinion of the writers on how some of the specifics should be

designed. For example, and relevant to this case, a structural engineer and a pavement engineer may both be tasked with designing a concrete slab-on-ground for a hangar foundation and may both design a well-performing slab that supports the loads and is economical and durable, but may have drastically different approaches on how to achieve that. More specifically, a structural engineer tends to approach the design of a slab-on-ground by adding steel reinforcement to resist flexure in the slab due to the given loads. They may also place the reinforcement in a way that controls cracking, but does not prevent it. A pavement engineer would likely approach the design differently by placing steel at mid-depth, not to add strength or prevent flexure, but purely to slow the deterioration of cracks in order to prevent FOD hazards. Furthermore, a military pavement engineer, most like the kind that would design a slab-on-ground for use in a hangar, would tend to design with yet another approach. They typically would approach the design task by using no reinforcement at all, but would rather use a much thicker slab design based on research conducted by the Corps of Engineers (COE), which proved that steel reinforcement, while it did slow the deterioration of a crack, did nothing to prevent the formation of a crack (Donnally, 2016). This begs the question: which approach is the right approach or rather which one produces the all-around better slab? The differences in approaches are evident in the differences in the current code specifications and design guides. This portion of the literature review, in addition to the historical review in Chapter 3, discusses the specifics of what makes each code or design guide different.

Organizations whose code specifications and design guides are reviewed in this thesis include the ACI, the PCA, and most relevant to this research, the UFC, which replaced the former Technical Manuals (TM) and Air Force Manuals (AFM), which are also referenced in this thesis. ACI has over 300 technical documents including code specifications and design

guides. Some are more general and many of them cover very specific topics depending on the design application of the member. Relevant to this research are ACI 302.2R: Guide for Concrete Slabs that Receive Moisture-Sensitive Flooring Materials, ACI 302.1R: Guide for Concrete Floor and Slab Construction, ACI 544: Fiber Reinforced Concrete, and ACI 360R: Guide to Design of Slabs-on-Ground. The last guide is discussed in detail this thesis. Relevant military documents include UFC 3-260-06: Pavement Design for Airfields and UFC 3-320-06A: Concrete Floor Slabs on Grade Subjected to Heavy Loads, which replaced ARMY TM 5-809-12 and AIR FORCE AFM 88-3, chapter 15 in the early 2000's. These two UFCs are reviewed in depth in the following chapters.

ACI 360R contains a chart that originated from the COE detailing how to select the thickness of reinforced slabs-on-ground. As previously described in this literature review, thickness has much to do with the cracking behavior of concrete slabs-on-ground. The nomograph, shown in Figure 2-2, compares the thickness of reinforced concrete pavement, h_r and the thickness of plain concrete pavement, *h*, against the cross sectional area of the steel, A_s, the maximum allowable length of the concrete slab, L, and the percentage of steel in the slab, s %. A nomograph is a tool that allows a designer to compare three or more variables at once by drawing a line connecting known values in order to find unknown values. The challenge lies in the fact that these charts have been used for over 70 years, so it is reasonable to question whether the nomograph still uses a computing methodology that is up-to-date with current state-of-the-art technology.

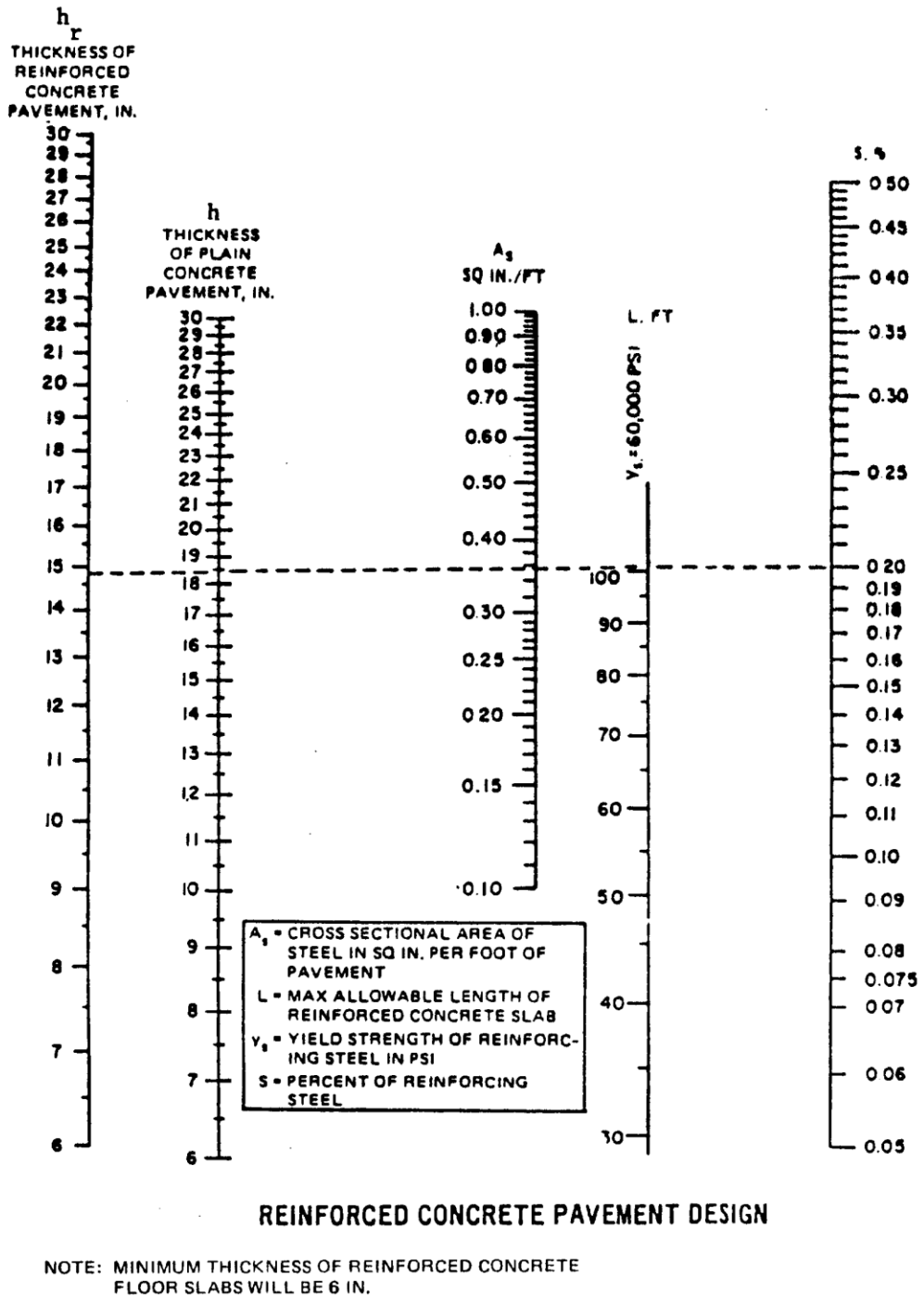

Figure 2-2: Nomograph of Design Thicknesses for Reinforced Floor Slabs (ACI 360R-10)

Published in 2007, "ACI 360R-06 Brings Slabs on Ground Design into the 21st Century", author and structural engineer Arthur W. McKinney identifies what improvements are needed in

the design and analysis of slabs-on-ground and reviews the updates made within the 15-year gap between the 1992 and 2006 versions of ACI 360R. ACI considers slabs-on-ground as non-structural. In order to determine the required section modulus and thickness of slab, an appropriate factor of safety or modulus of rupture must be applied. McKinney states that joint spacing should be selected based only on the selected slab thickness, which is one of the most relevant features of this research project, and that reinforcement of concrete slabs-on-ground may allow for the elimination of contraction joints (McKinney, 2007). For this reason, the 2006 version of ACI 360R proposes the alternative method of the introduction of light reinforcement continuous through the contraction joints. Also in the new ACI version, the notion that fibers contribute to ductility is no longer supported since they do not justify extending joint spacing or reducing slab thickness. McKinney also discusses the fact that the 1992 version of ACI 360R considers subgrade friction as the primary cause of concrete cracking, while the 2006 version considers curling and/or warping as the primary cause. Lastly, McKinney concludes that one of the main focuses of designing a slab-on-ground is that the design should provide an adequate thickness and that joints should be closely spaced with adequate provision for load transfer. As an alternative, the that joints should be either minimized by shrinkage-compensating concrete or eliminated by post-tensioned or heavy, continuous reinforcement. Finally, the design of a slab-on-ground must be reconciled with the actual means, methods, materials, and site conditions of the project.

ACI 302.2R, a guide on moisture-sensitive slabs, also discusses slab thickness in depth. The first eight chapters cover the drying process and effects of moisture on concrete. Within ACI 302.2R, the ninth chapter provides recommendations to improve performance for slabs in contact with moisture and alkalinity and also discusses the principles behind reinforced slab

thickness design. More general than ACI 302.2R is ACI 302.1R: Guide for Concrete Floor and Slab Construction. This publication purports that it is unrealistic to expect a non-prestressed slab to never experience cracking (ACI 302.1R), and states that the performance of the slab, as we know from Westergaard's theory, depends on both the soil support system and the slab itself. Knowing that cracks are unavoidable in non-prestressed slab-on-ground designs, ACI 302.1R aims to explain what causes cracking and how to avoid or limit it. This includes the discussion of reinforcement, joint design, mix design, and curing. According to the guide, which is based on decades of research, cracks are caused by the restraint of volume change. The restraint of the shrinkage that occurs with drying, the contraction and expansion as the temperature changes, curling at the slab edge, settlement of the soil beneath the slab, and the applied loads (ACI 302.1R) causes stresses in the slab which result in cracking. The suggestions to mitigate the issues that surround cracking include placing temperature and shrinkage reinforcement within the upper one third of the slab thickness, based on lab experiments. As explained in the code, reinforcement is used to control cracks by controlling their width, but does not prevent cracking. Other suggestions to mitigate cracking issues include using a vapor barrier, something which is discussed thoroughly in ACI 302.2R and explained in the following paragraph.

A vapor barrier is typically a plastic sheet that is placed over the subgrade before the placement of the slab. The barrier protects the concrete slab from absorbing and retaining moisture from the ground and causing issues with molding in the interior of the building or, in our case, the hangar. Lstiburek (2008) describes common vapor barrier mistakes and the very simple ways of fixing them. Lstiburek explains why a vapor barrier is necessary, also stated in guides such as ACI 302, and places emphasis on the common mistake of placing the vapor barrier below the concrete slab and adding a layer of sand in between the two. The idea came

from constructors in California who believed that they could prevent or reduce curling in the slab by using the sand layer to make the drying process more even, since uneven drying can cause slab curling (Lstiburek, 2008). The best way to prevent slab curling is to use a low water-to-cement (w/c) ratio. According to Lstiburek, a w/c less than 0.5 should be used, combined with using wetted burlap to "wet cure" the top of the concrete (Lstiburek, 2008). That method prevents moisture from being trapped under the concrete slab in the sand slayer, because unfortunately, a vapor barrier does work two ways. The vapor barrier not only prevents moisture from the subgrade from being absorbed into the concrete slab, but also prevents excess water held in a sand layer from draining out.

Lstiburek (2012) also explains issues with thermal cracking and discusses the benefits of a vapor barrier in that application. Preventing unnecessary moisture in a concrete slab-on-ground via the use of a vapor barrier also helps mitigate issues with thermal cracking. When water gets into the tiny hairline cracks in a concrete slab and freezes, the cracks get bigger, causing further crack deterioration leading to potential FOD hazards. Lstiburek describes where to place not only the vapor barrier, which is just under the concrete slab with no sand layer, but also where to place thermal insulation to mitigate that hazard.

The United States military adheres to their own set of standards. Each one of the five branches of the military (U.S. Military: Air Force, Army, Coast Guard, Marine Corps, and Navy) previously created and used their own technical documents. This was a problem because of potential discrepancies and thus limiting interoperability between the branches and services. To overcome such limitations, each branch came together and created the Unified Facilities Criteria, which provides criteria and standards for the entire Department of Defense (DoD).

The military code UFC 3-320-06A: Concrete Floor Slabs on Grade Subjected to Heavy Loads, serves as a good resource for the design of concrete slabs in hangars. UFC 3-320-06A covers every area of the design of slabs subjected to heavy loads. Considering the immense weight of the aircraft typically stored in a military hangar, it is invaluable to have a set of design criteria that addresses specifically slabs-on-ground subjected to heavy loads. The manual defines heavy loads as loads that are compliant with any of the following: moving live loads that exceed a forklift axle load of five kips or 5,000 pounds, stationary live loads that exceed 400 pounds per square foot, or concentrated wall loads that exceed 600 pounds per linear foot.

Moving live loads are loads imposed by vehicular traffic. These could include machinery such as forklifts that may be carrying heavy materials as well as the weight of the aircraft stored in the hangar. These types of loads are considered wheel loads, which are idealized as a point load on the slab at all places where a wheel makes contact with the concrete. Stationary live loads are loads imposed by items not in motion at the time, but also not attached to the slab, so that they can be moved. A wall load is a load imposed by either a wall or a partition (UFC 3-320-06A). Dr. Robert Dinan of the Air Force Civil Engineer Center (AFCEC) working to update UFC 3-320-06A pointed out several points of possible concern within the manual. The chapter on stationary live loads contains a table stating the maximum allowable stationary live loads included here as Table 2-1, along with Figure 2-3. The factor of safety (FS) used to compute the values in the table is not explicitly stated, but Dr. Dinan and his team clarified that the FS used was equal to 2 since the code calls for a stress ratio of one half of the allowable extreme fiber stress, which is assumed to be equal to one half of the normal 28-day flexural strength of the concrete. Dr. Dinan also raised concern with the calculation of the constant subgrade modulus factors. These moduli are shown in Table 2-2. The team determined that the *k* factors were valid

because the load-induced slab stress is proportional to the modulus of subgrade reaction assumed in Table 2-1, which was equal to 100 lb/in^3 as described in the note below Table 2-1.

Table 2-1: Maximum Allowable Stationary Live Loads (UFC 3-320-06A)

Slab Thickness, *h* (inches)	Stationary Live Load, *w* (in-lb/ft^2) for These Flexural Strengths of Concrete			
	550 lb/in^2	600 lb/in^2	650 lb/in^2	700 lb/in^2
6	868	947	1,026	1,105
7	938	1,023	1,109	1,194
8	1,003	1,094	1,185	1,276
9	1,064	1,160	1,257	1,354
10	1,121	1,223	1,325	1,427
11	1,176	1,283	1,390	1,497
12	1,228	1,340	1,452	1,563
14	1,326	1,447	1,568	1,689
16	1,418	1,547	1,676	1,805
18	1,504	1,641	1,778	1,915
20	1,586	1,730	1,874	2,018

*Note: Stationary live loads tabulated above are based on a modulus of subgrade reaction (k) of 100 lb/in^3. Maximum allowable stationary live loads for other moduli of subgrade reaction is computed by multiplying the above-tabulated loads by a constant factor. Constants for other subgrade moduli are tabulated below in Table 2-2.

Table 2-2: Constant Subgrade Moduli (UFC 3-320-06A)

Modulus of Subgrade Reaction (pci)	25	50	100	200	300
Constant Factor	0.5	0.7	1	1.4	1.7

*For other modulus of subgrade reaction values, the constant values may be found from the expression $\sqrt{k/100}$.

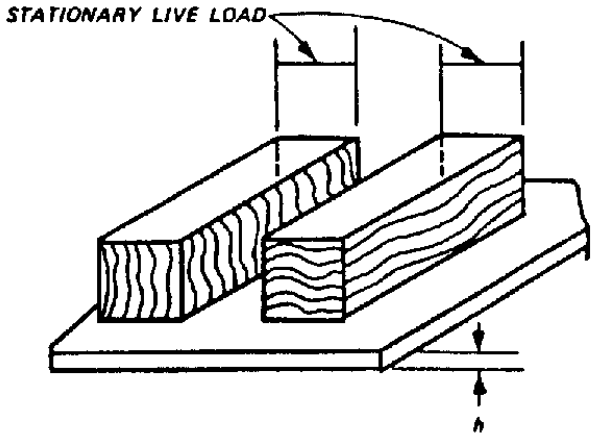

Figure 2-3: Diagram of the Stationary Live Load Set-up Used for Calculations in Table 2-1 (UFC 3-320-06A)

In determining whether Tables 2-1 and 2-2 are still valid, the team proved that tables similar to these were included in PCA manuals, which were copied into ACI 360, but did not include thicknesses as deep as what is included in Table 2-1 (Dinan, 2016). A third table was brought into question, included here as Table 2-3 along with Figure 2-4, which defines the minimum thickness of thickened floor slabs for wall loads near the center of a slab or near keyed or doweled joints. This table could not be found in other manuals (Dinan, 2016) and is considered specific to applications of concrete slabs-on-ground subjected to heavy loads.

Table 2-3: Minimum Thickness of Thickened Floor Slab for Wall Load near Center of Slab or near Keyed or Doweled Joint (UFC 3-320-06A)

Thickness of Thickened Floor Slab, t_e (inches)	Slab Line Load Capacity, P (lb/lin. ft)			
	Flexural Strength of Concrete (lb/in^2)			
	550	600	650	700
4	425	455	485	510
5	565	600	640	675
6	710	755	805	850
7	860	920	975	1,030
8	1,015	1,080	1,150	1,215
9	1,175	1,255	1,330	1,410
10	1,340	1,430	1,520	1,605

*Note: The allowable wall loads are based on a modulus of subgrade reaction, k, of 100 lb/in^3. The thickness of the thickened slab is computed by multiplying the above thickness by a constant factor as shown in Table 2-4 below.

Table 2-4: Modulus of Subgrade Reaction Constant Factors (UFC 3-320-06A)

Modulus of Subgrade Reaction, k (lb/in^3)	25	50	100	200	300
Constant Factor	1.3	1.1	1	0.9	0.8

*Note: For other modulus of subgrade reaction values the constant values may be found from $\sqrt{100/k}$. For this application the flexural strength of concrete was assumed equal to $9\sqrt{f_c'}$ where $f_c^{'}$ is the specified compressive strength of concrete (lb/in^2).

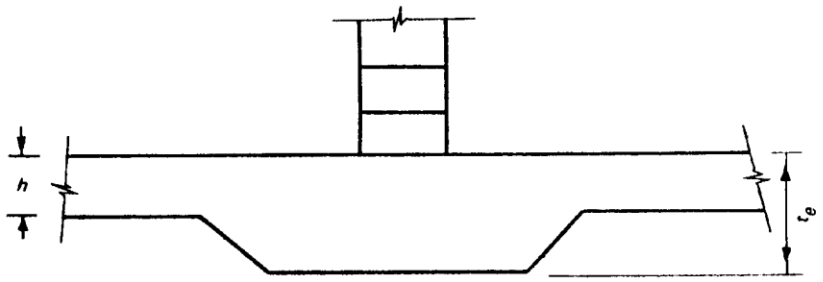

Figure 2-4: Diagram of Thickened Slab for a Wall Load (UFC 3-320-06A)

Dr. Dinan (2016) also raised concern with the modulus of subgrade reaction values, k, used in Table 2-5. For these calculations, a geotechnical engineer on a construction project is typically the one to determine the k value in situ by performing a site exploration, therefore the accuracy of the k values used in Table 2-5 would depend on the site subgrade. Table 2-5 shows the modulus of subgrade reaction for several soil types under certain moisture content (shown as a percentage).

Table 2-5: Typical Values of Modulus of Subgrade Reaction (UFC 3-320-06A)

Types of Materials	**Modulus of Subgrade Reaction, k (lb/in^3)**							
	1-4%	5-8%	9-12%	13-16%	17-20%	21-24%	25-28%	Over 29%
Silts and clays w/ Liquid limit > 50 (OH, CH, MH)	--	175	150	125	100	75	50	25
Silts and clays w/ Liquid limit < 50 (OL, CL, ML)	--	200	175	150	125	100	75	50
Silty and clayey sands (SM & SC)	300	250	225	200	150	--	--	--
Gravelly sands (SW & SP)	300+	300	250	--	--	--	--	--
Silty and clayey gravels (GM & GC)	300+	300+	300	250	--	--	--	--
Gravel and sandy gravels (GW & GP)	300+	300+	--	--	--	--	--	--

Other concerns included whether the nomograph in Chapter 5 of the UFC, the chapter on design procedures is currently valid. The nomograph is the same as the one in ACI 360, Figure 2-1, for determining the thickness of concrete slabs-on-ground in pavement/hangar applications. A second nomograph of concern, shown as Figure 2-5, compares k values with slab thickness and the flexural strength of the concrete along with a design index ranging from one to ten. The design index is defined in Chapter 4.

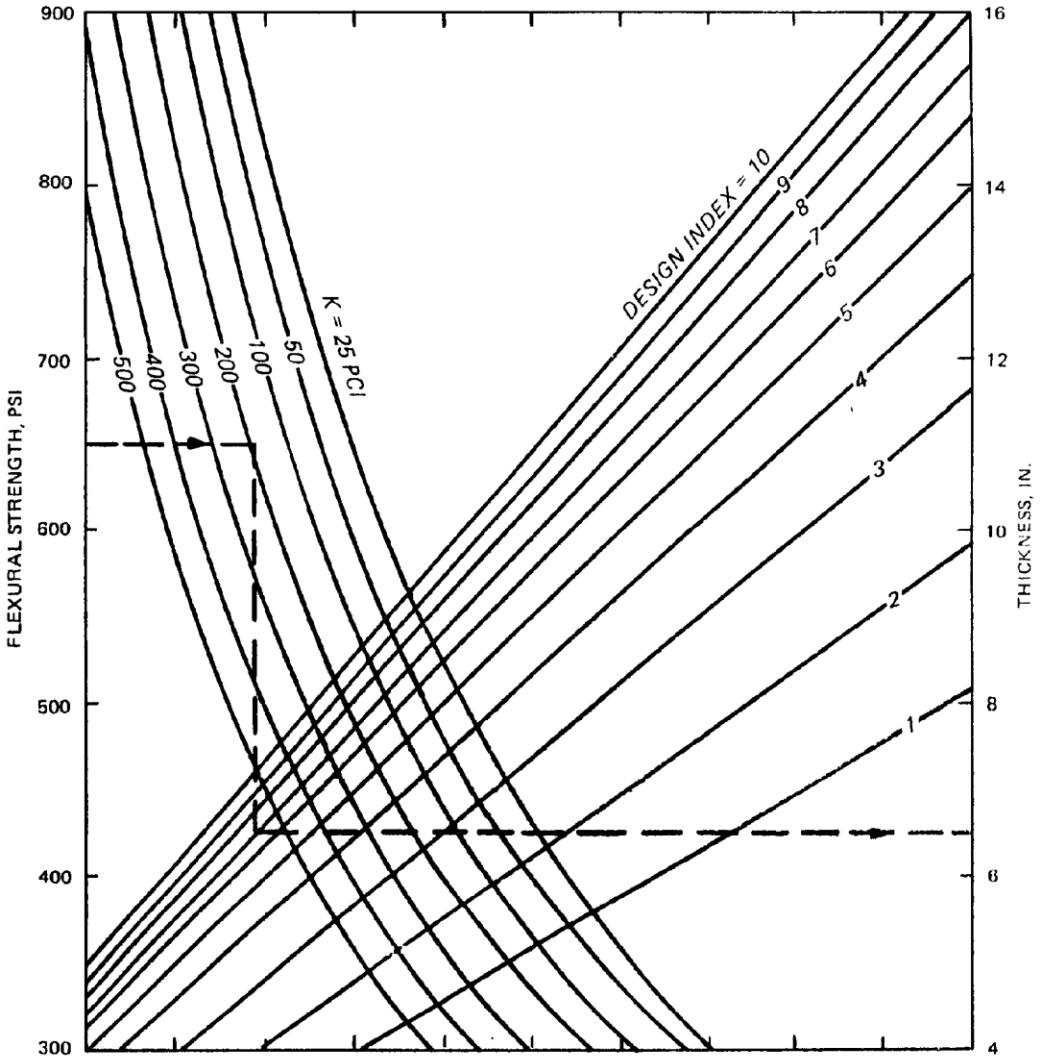

Figure 2-5: Design Curves for Concrete Floor Slabs by Design Index (UFC 3-320-06A)

The current validity, as well as the origins of both Figure 2-1 and 2-5, required further exploration. This could be in the form of performing calculations to attempt to match the values shown in the charts and comparing them with current state-of-the-art technology and knowledge of slabs-on-ground. It is also important to note that the charts were adopted from pavement design procedures, so further research into the references within UFC 3-320-06A may be helpful. Other exploratory ideas include reconciling the values within the charts with other UFCs on

airfield runways and hangar floors as well as with PCASE (Pavement-Transportation Computer Assisted Structural Engineering) methodologies, a pavement engineering software tool.

The final discrepancies lie within the appendices of UFC 3-320-06A. In Appendix B of the manual, there is a lack of clarity in the factor of safety used in the equations for computing the allowable wall load near a free edge. In addition, there is the use of a modulus of rupture that may be too low. In Appendix C of the UFC, there are four example calculations that need to be reviewed to ensure relevancy (Dinan, 2016). Overall, there seems are many unknowns within the manual.

2.5 PAST AND CURRENT RESEARCH ON SLABS-ON-GROUND

The above-described methods for the design of concrete slabs-on-ground are further described in an organized and comprehensive manner in *Designing Floor Slabs On Grade* by Boyd C. Ringo and Robert B. Anderson (1996). The book serves as a "step-by-step" guide complete with example calculations for designing concrete slabs-on-ground using six common methods including the following:

1. The Portland Cement Association (PCA) method
2. The Wire Reinforcement Institute (WRI) method
3. The Post-Tensioning Institute (PTI) method
4. The United States Army Corps of Engineers (COE) method
5. The United States Army and Air Force (UFC, formerly known as TM) method
6. The American Concrete Institute Committee 223 Standard Practice (ACI 223)

ACI 360R: *The Design of Slabs-on-Ground* is not mentioned as a method for slab thickness selection in the Ringo and Anderson book. For the purpose of this thesis, the PCA method, the COE method, the Air Force (UFC) method, and the ACI 360R methods were

considered. They are the most relevant to the application of slabs-on-ground in hangars. Example calculations and an in-depth comparison and discussion for each of these methods are presented in Chapter 4.

It is important to be meticulous in the selection of a slab-on-ground thickness because it can determine the performance and longevity of the slab. This is not an easy task, however, considering the complexity of inputs and considerations in selecting slab thickness such as the variety of loads and environmental effects (Delatte, 2008). The loads to which a slab-on-ground is subjected one day may be very different from those for the following day. This difference can come in the form of an increase or decrease in load or in the form of a change in the location of load application. Delatte (2008) suggests a combination of theoretical analysis, an analysis of experimental data, and a study of pavement or slab performance under service-load conditions when designing a slab-on-ground. Feldmann and Schambach (2016) explain that the purpose of the slab, in addition to the loads it must carry, and the applicable standards, plays a key role in which method should be used for selecting slab-on-ground design thickness. For example, there exist certain minimum slab thickness requirements depending on the applicable code specifications.

CHAPTER 3: HISTORICAL TIMELINE OF THE DESIGN AND ANALYSIS OF SLABS-ON-GROUND

3.1 OVERVIEW

Figure 3-1 illustrates a timeline of events describing the development of the process of analyzing slabs on grade beginning with Winkler's theory of subgrade behavior (1868) and ending with findings by Ioannides et al. (1984). The events depicted in Figure 3-1 represent the most important details in the history of the analysis of slabs-on-ground in relation to this research. The most important individuals in relation to this research have been included and bolded in the figure.

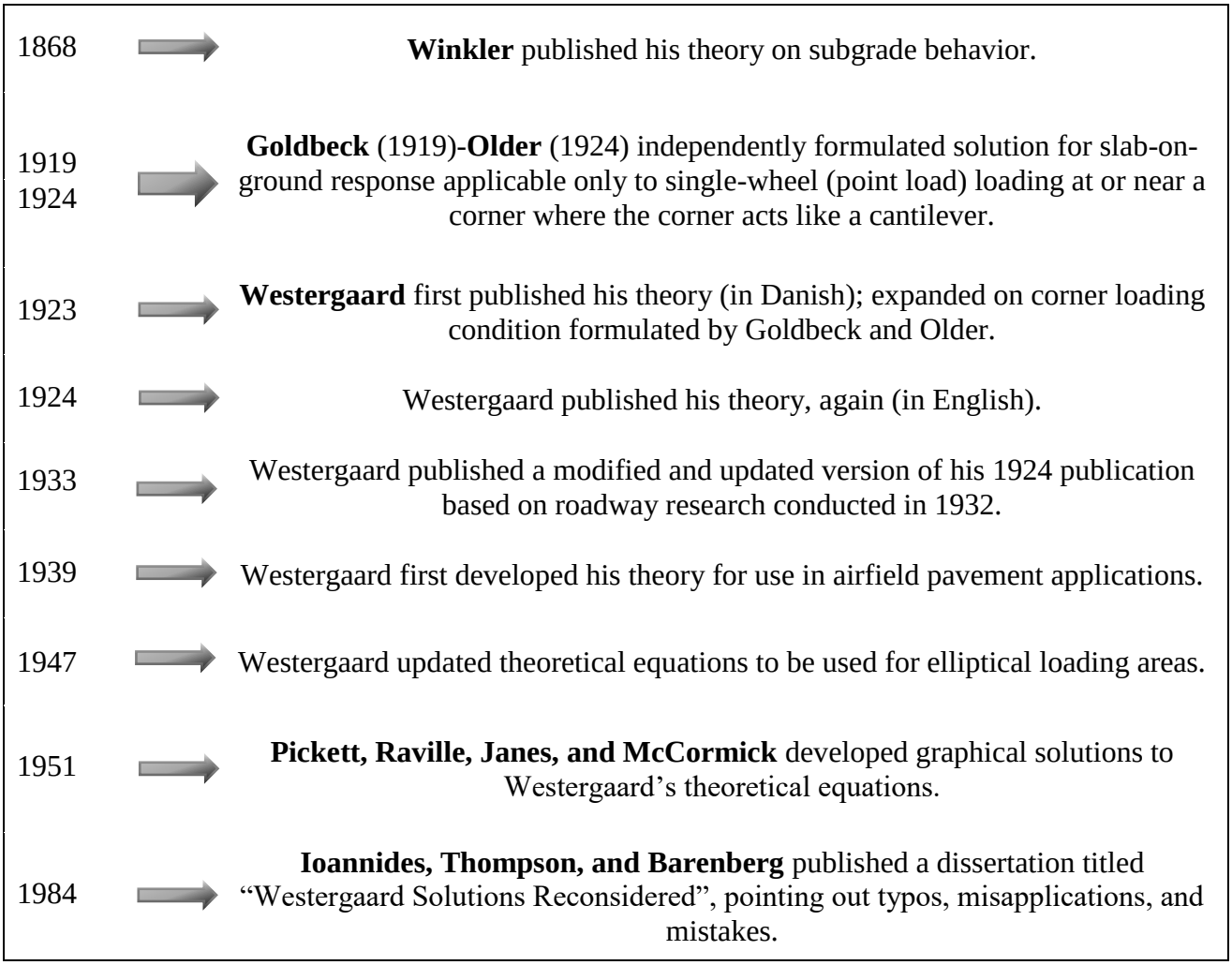

Figure 3-1: Historical Timeline of the Analysis of Slabs-on-Ground

The following section provides an in-depth discussion on each of the events in the timeline. In addition, there are publications by some of the same authors and publications by others that are briefly mentioned in the proceeding section.

3.2 ORIGINS OF SLAB-ON-GROUND DESIGN AND ANALYSIS THEORY

3.2.1 WINKLER BEAM THEORY

Emil Winkler was an engineer born in a historical region of central European region (current Poland) called Silesia in 1835 (Frýba, 1995). His most notable work was the

development of a theory surrounding subgrade reactions. Winkler's research revolved around the mechanics of an elastic beam resting on infinitely many linear springs acting perpendicularly to the span of the beam and acting parallel to the application of a load as depicted in Figure 3-2.

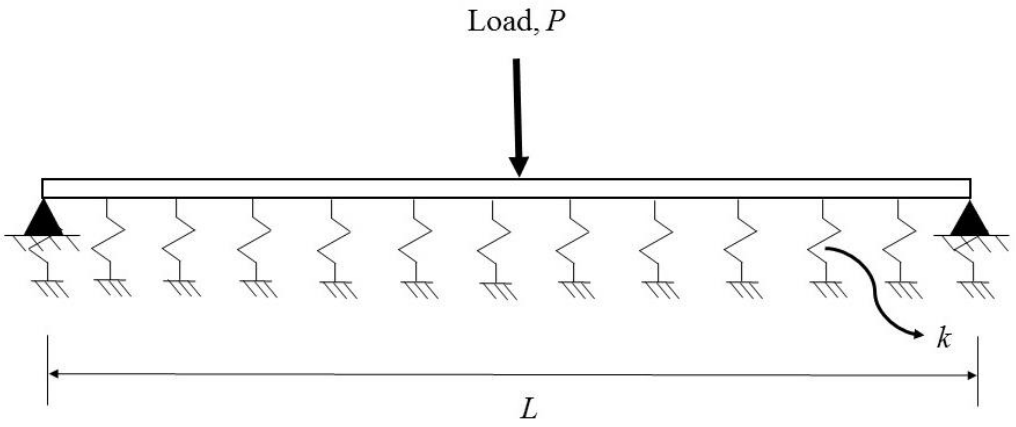

Figure 3-2: Winkler Beam Theory

Winkler theorized the behavior of beams on foundations as a beam of length, L, acting on a subgrade having a proportionality constant, k, called the modulus of subgrade reaction. Each spring behaves independently of the other (Ioannides, 1984). The modulus of subgrade reaction is dependent on the physical properties of the foundation, and in this case, the soil on which the beam is resting. This proportionality constant is based on the idea that the ratio of contact pressure to deflection is the same at every point of the beam (Winkler, 1868). Winkler referred to the behavior of this idealization of subgrade as behaving like a "dense liquid". This is in contrast to the behavior of the subgrade as behaving like an "elastic solid". As described by Brink (2003), elastic solid behavior is similar to the behavior of a beam or plate resting on an elastic rubber foundation. Pickett, among others, later refuted Winkler's theory of subgrade

behavior in 1951. Pickett et al. (1951) asserted that the soil or subgrade beneath a beam or slab behaves more like an elastic solid than a dense liquid. This is evident in Figure 3-3 from (Hammons and Ioannides, 1996), which shows the difference in behavior between a Winkler foundation and an elastic solid foundation.

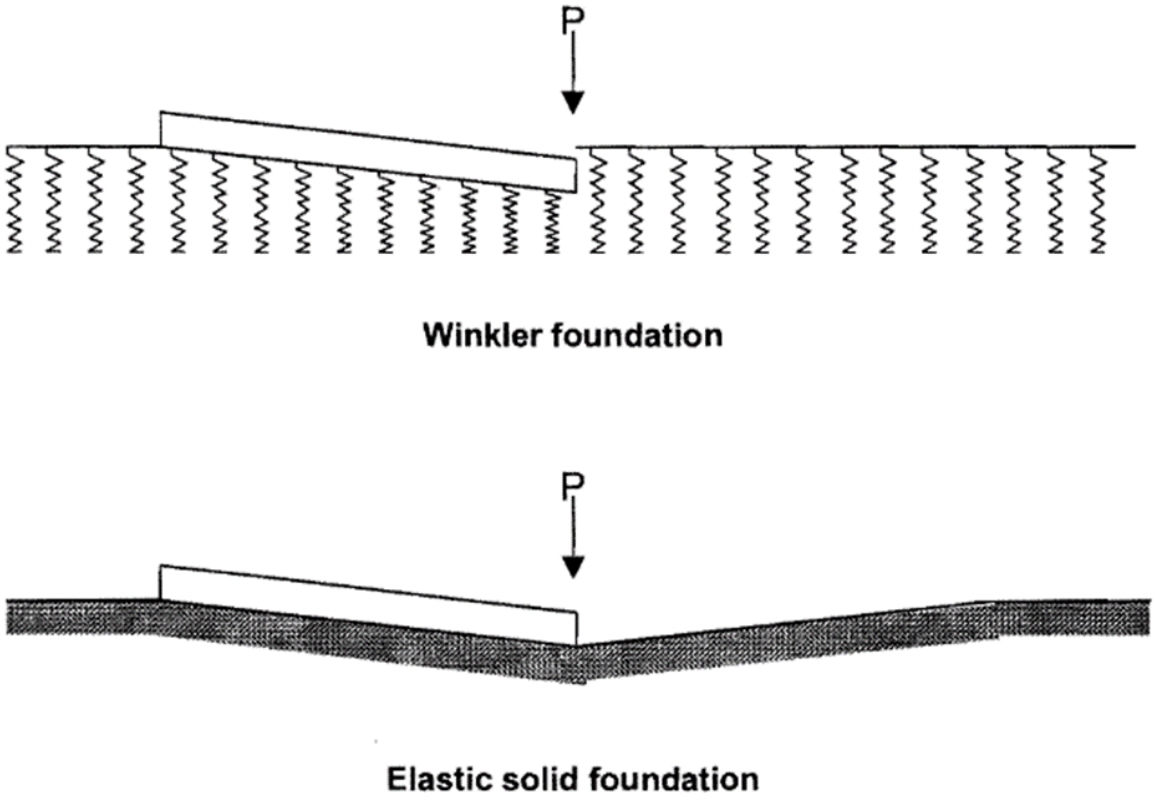

Figure 3-3: Behavioral Difference between a Winkler Foundation (Dense Liquid) and an Elastic Solid Foundation (Hammons and Ioannides, 1996)

The main difference lies in the dependency of each "spring" to one another. In Winkler's subgrade theory, the springs each react and displace independently of one another. Elastic solid foundation theory rests on the idea that the subgrade or soil can be thought of as an infinite number of springs acting side by side, whose reactions and displacements are dependent on each other. This is particularly important at edge and corner loadings where a member ends yet the

foundation continues. As discussed in Section 3.2.3, Westergaard eventually took Winkler's theory a step further by applying it in the case of slabs-on-ground which can be described as a three-dimensional version of Winkler's theory (ACI Committee 360, 2010).

3.2.2 THE GOLDBECK-OLDER EQUATION

Former director of the Bureau of Public Roads, A. T. Goldbeck in 1919, and Clifford Older of the Illinois Highway Department in 1924 independently developed equations to describe stress and deflection in the case of point loading at or near the corner of a slab-on-ground (Ioannides et al., 1985). In the Goldbeck-Older equation, (Equation 3-1), it is assumed that this type of loading results in the corner of the slab-on-ground behaving similar to a cantilever beam, effectively assuming a modulus of subgrade reaction of zero. Thus, the equation results from the application of basic mechanics of materials. The corner stress is calculated across a failure cross section that is a distance *c* from the corner, represented by *x* in the figure, with a fracture length of $2x$, where the moment of inertia for this failure plane, I, is calculated as shown in Equation 3-2. The base, b, of the failure plane is represented in Figure 3-4 as length $2x$ and the height, h, is represented by the thickness, t, of the slab. Given a load, P, the moment, M, is equal to Px. Inserting the values known for M, c, and I, the stress in a corner-loading scenario is equal to a value of $3P$ divided by the thickness squared.

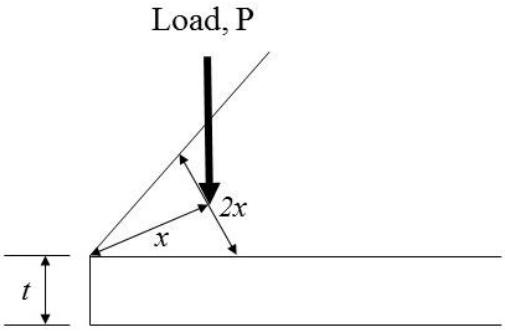

Figure 3-4: Illustration of the Goldbeck-Older Corner-Loading Theoretical Set-Up

$$\sigma_{corner} = \frac{Mc}{I} = \frac{3P}{t^2} \tag{3-1}$$

$$I = \frac{bh^3}{12} \tag{3-2}$$

3.2.3 WESTERGAARD PLATE THEORY

Harold M. Westergaard was a structural engineer originally from Denmark. Not long after the publication of the works of Goldbeck and Older, Westergaard developed his own equations for stresses and deflections in slabs-on-ground not only for the corner-loading situation, but also for edge and interior-loading scenarios. His equation for stress for a corner-loading situation was an improvement on the Goldbeck-Older equation (Delatte, 2008). Westergaard took Winkler's subgrade research a step further when he applied the research to slabs-on-ground. Westergaard's research expanded on Winkler's studies of beams on elastic foundations, which experience one-way bending, and applied it to the two-way bending that occurs in slabs-on-ground. According to Huang (1996), Westergaard's equations serve as the

most extensive theoretical studies on the stresses and deflections of concrete slab-on-ground pavements.

First published in Danish in 1923, some of which are still used today, Westergaard's research produced three stress and three deflection equations, a set of stress and deflection equations for each loading condition. Often referred to as "The Westergaard Equations" or "Westergaard Solutions", admittedly vague titles considering the many areas in which Westergaard conducted research, the equations are applicable in three loading conditions: interior, edge, and corner loading and assume a slab-on-ground of infinite or semi-infinite dimension (Ioannides et al., 1984). Westergaard's work also extended into the area of temperature curling and concrete crack analysis (Huang, 1996). Figures 3-5 through 3-7 show each of the three loading conditions for which Westergaard developed his equations.

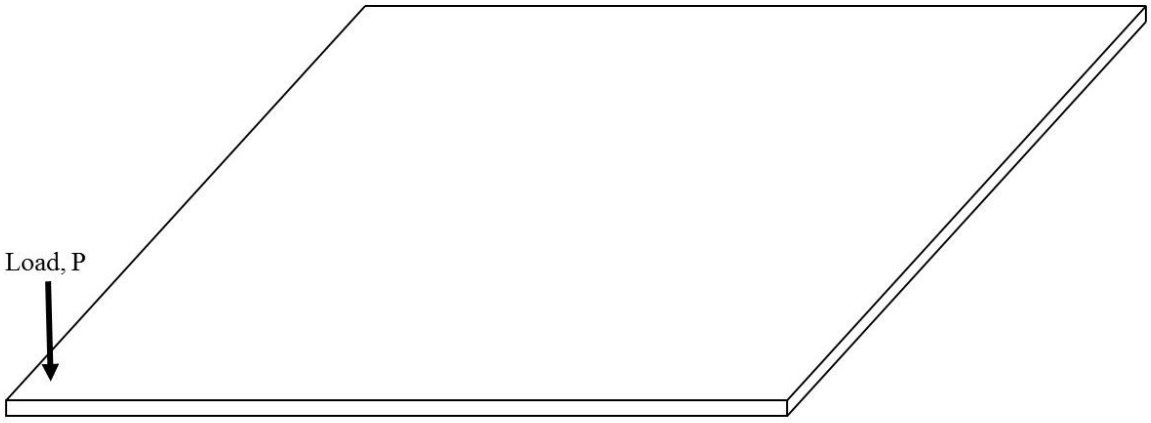

Figure 3-5: Corner-Loading Example

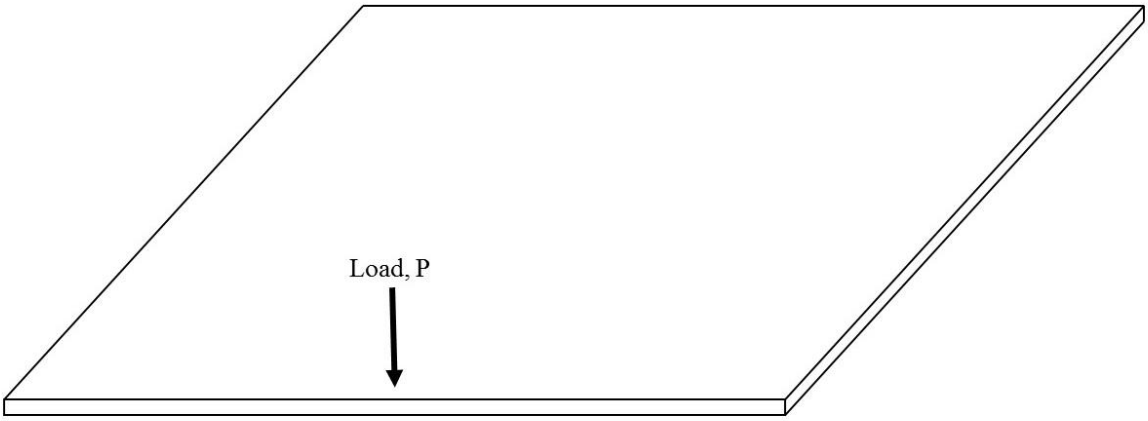

Figure 3-6: Edge Loading Example

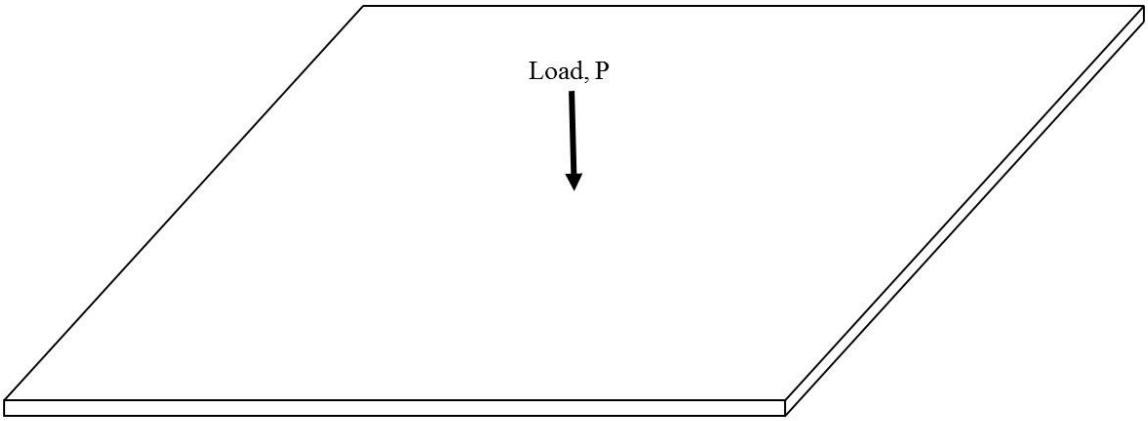

Figure 3-7: Interior Loading Example

As pointed out by Pickett et al. (1951), the equations for stress and deflection are limited in the sense that a load may be applied anywhere at any given time and may even include more than one load. This is especially true in the case of airplane hangars because airplanes have at least three points on contact on the pavement at all times. This point is discussed further in

Section 3.2.4. Slabs-on-ground are often built in segments consisting of smaller slabs connected by joints. Anywhere a joint connects slab segments, there can be edge or corner loading conditions if the wheel load is in the vicinity of a joint. The interior loading condition applies to when the wheel load is a considerable distance from a joint.

Westergaard updated the Goldbeck-Older equation for stress under a corner loading including a reduction factor in the form of the value between the brackets in Equation 3-3 (Westergaard, 1924). It is important to note that the equation applies only to circular loading areas, where a represents the radius of that circle. Outside of the brackets, there is no difference in the Westergaard equation and Goldbeck-Older equation for corner loading. The reduction factor is dependent not only on the size of the loading area, but also the radius of relative stiffness, l. Calculated using Equation 3-4, the radius of relative stiffness is a function of the modulus of elasticity and Poisson's ratio of the concrete, E and ν, respectively, as well as the thickness, t, of the slab and the modulus of subgrade reaction, k. The radius of relative stiffness is the relative stiffness of the slab to the subgrade and is equal to the fourth root of the plate rigidity, *D*, divided by the modulus of subgrade reaction, *k*. The flexural rigidity of the plate is calculated using Equation 3-15. Originally published in 1924, Equation 3-3 would be later updated by Ioannides et al. (1984) as described in Section 3.2.5. Furthermore, Westergaard developed an equation for the deflection of a slab in the case of corner loading. Using Ritz's successive approximation method, Westergaard published Equation 3-5 in 1924 (Westergaard, 1924). The equation is a function of the modulus of subgrade reaction, the radius of relative stiffness, and the radius of loading area.

Stress Equation for the Corner Loading Condition (Circular Load Area):

$$\sigma_{corner} = \frac{3P}{t^2}[1-(\frac{a_1}{l})^{0.6}] \quad (3\text{-}3)$$

Where $a_1 = \sqrt{2}a$

Radius of Relative Stiffness for a Dense Liquid Subgrade, $l = \sqrt[4]{\frac{D}{k}} = \sqrt[4]{\frac{Et^3}{12(1-\nu^2)k}}$ (3-4)

Deflection Equation for the Corner Loading Condition (Circular Load Area):

$$\delta_{corner} = \frac{P}{kl^2}\left(1.1-0.88\frac{a_1}{l}\right) \quad (3\text{-}5)$$

When deriving stress equations for the interior loading condition, Westergaard noted the need for a different equation for both ordinary and special theory (Westergaard, 1924). Ordinary theory involves the idea that plane sections remain plane while special theory does not. Special theory is required at locations in the slab-on-ground that are immediately near the concentrated load. The Equations 3-6 and 3-8 are stress equations for interior loading for both ordinary and special theory, respectively. They are intended only for circular loading areas. There exists an equivalent loading area denoted by a radius of loading area, b. Westergaard defines this radius as Equations 3-7 and 3-9 (Westergaard, 1924). Whenever the ordinary loading area radius, a, is less than 1.724 times the thickness, the special theory equation must be used to calculated the stress under the interior loading condition. Substituting Equation 3-9 for *b* in Equation 3-6 yields Equation 3-8, which is the special theory Westergaard stress equation for the interior loading condition. Equation 3-10 represents the deflection of a slab-on-ground under the same loading condition.

Stress Equations for the Interior Loading Condition (Circular Load Area):

Ordinary Theory:

$$\sigma_{interior} = \frac{3(1+\nu)P}{2\pi t^2}\left(\ln\left(\frac{l}{b}\right)+0.6159\right) \tag{3-6}$$

$$b = a \quad \text{When} \quad a \geq 1.724t \tag{3-7}$$

Special Theory:

$$\sigma_{interior} = 0.3162\frac{P}{t^2}\left(\log\left(t^3\right)-4\log\left(\sqrt{1.6a^2+t^2}-0.675t\right)-\log\left(k\right)+6.478\right) \tag{3-8}$$

$$b = \sqrt{1.6a^2+t^2}-0.675t \quad \text{When} \quad a < 1.724t \tag{3-9}$$

*Note: b has already been inserted into Equation 3-8

Deflection Equation for the Interior Loading Condition (Circular Load Area):

$$\delta_{interior} = \frac{P}{8kl^2}\left\{1+\frac{1}{2\pi}\left[\ln\left(\frac{a}{2l}\right)-0.673\right]\left(\frac{a}{l}\right)^2\right\} \tag{3-10}$$

The edge-loading condition equations for stress and deflection are shown in Equations 3-11 and 3-12, respectively. The same assumptions and equations used to calculate the equivalent radius, b, from the interior-loading condition apply to the edge-loading condition as well. Westergaard attributes this as being due to the similarity of the distribution of energy due to vertical shear stress in the corner and edge-loading scenarios (Westergaard, 1925).

Stress Equation for the Edge Loading Condition (Circular Load Area):

$$\sigma_{edge} = 0.572\frac{P}{t^2}\left[\log\left(t^3\right)-4\log\left(\sqrt{1.6a^2+t^2}-0.675t\right)-\log k+5.767\right] \tag{3-11}$$

Deflection Equation for the Edge Loading Condition (Circular Load Area):

$$\delta_{edge} = -\frac{1}{\sqrt{6}}(1+0.4\nu)\frac{P}{kl^2} \tag{3-12}$$

Westergaard published another report in 1939, which applied these equations for stress and deflection in slabs-on-ground to airfield pavement calculations. He asserted that although airplane wheels' contact areas and loads were significantly larger than those of roadway vehicles, these equations from 1924 still applied (Westergaard, 1939). Based on a growing number of research endeavors on the topic, Westergaard also presented an estimate for maximum stress if the equations had been based on the assumption of a deep elastic solid rather than a dense liquid.

In 1947, Westergaard published "New Formulas" for computing the stresses and deflections in slabs-on-ground under edge loading conditions. These equations were applicable for semi-circular loading areas at the edge (Westergaard, 1947), which were considered to be a more accurate representation of the actual loading area when compared to circular loading areas (Pickett et al., 1951). His new equations were essentially simplifications of his original equations, based on new research.

Westergaard's work has shaped the way engineers design slabs-on-ground since 1924. Since then, various researchers realized some errors or room for improvement in Westergaard's original work and theorized some "modified" Westergaard equations in order to mitigate these errors. Westergaard himself even realized some improvements to be made before his death in 1950 as evident in his 1939 and 1947 papers. Over time, Westergaard's equations have occasionally been misquoted or misapplied due to the particular set of assumptions that must be met to utilize the equations (Ioannides et al. 1984). In the research paper, published by the Transportation Research Record, titled *Westergaard Solutions Reconsidered,* Ioannides et al. (1985) broke the issues up into four parts and proposed a remedy to each of the four issues. In summary, the paper defined the issues with Westergaard's equations or solutions as follows: typographical errors in some of the equations, incorrect equations for edge stress, room for

improvement in equations for corner loading responses, and finally, a lack of slab size requirements for the development of Westergaard loading responses (Ioannides et al., 1985). Research conducted by Eftis and Liebowitz (1972) determined that some of the errors in Westergaard's late 1930s equations for concrete crack analysis can be traced to an oversight in earlier research conducted by MacGregor (1935) on which Westergaard based his work. Other contributions to the analysis of slabs-on-ground include the work of G. Murphy published in the 1937 Iowa State College of Agriculture and Mechanic Arts. Murphy conducted research on the stresses and deflections of loaded rectangular plates on elastic foundations and compared his results to those of Westergaard and found good agreement (1937).

H. M. Westergaard produced many publications throughout his career and more so towards the end of his career. Around the 1920's, many publications came out written by Westergaard regarding many topics surrounding the concept of states of stress. In the proceedings from the 1924 Highway Research Board Annual Meeting, Westergaard published his findings from the previous year titled "Theory of Stresses in Road Slabs". In the short publication, Westergaard reviews his own experimentation and findings and suggests that further research be conduction to develop a theory in three areas. His own findings encompassed the effects on stress based on where a load is placed on a pavement and the stiffness of the subgrade and pavement. His findings can be applied to slabs-on-ground because they are essentially finite pavements. This is also applicable because the concrete slab-on-ground in question with respect to this research effort involves mostly wheel loading, like in pavements. Westergaard concluded that the size and shape of the contact area between and wheel and the slab as well as the distribution of pressure in this contact area have influence upon the maximum stress distributed in the slab. In addition, assuming a slab of constant thickness, a load placed at the edge results in

larger deflections and stress versus a load placed at a substantial distance away from the edge. Furthermore, a load that is placed at a corner produces tension at the top of the slab that is larger than the tension that the same load produces at the bottom of the slab if it were placed at a considerable distance from the corners and edge of the slab; the latter of which depends on the type of loading and the relative stiffness of the subgrade.

Concluding his research findings, Westergaard proposed the development of three theories. First, Westergaard proposed a theory concerning the state of stress due to a load distributed over a small area near the corner of a slab. Second, he proposed a theory that regards the influence of the gradual variation of thickness from one point to another. Lastly, Westergaard suggested further research into the dynamical action of slabs under impact loads from the viewpoint of the theory of vibrations. The work completed by Westergaard is what is considered to be "closed form solutions" (Krishna Rao, 2018), meaning that the equations are finite. The work conducted by Pickett et al. serves as a contrast because the solutions may be calculated using influence charts as described in the following section.

3.2.4 PICKETT, RAVILLE, JANES, MCCORMICK, AND RAY DEVELOP GRAPHICAL SOLUTIONS TO WESTERGAARD'S THEORETICAL EQUATIONS

Some engineers would disagree that the subgrade beneath a slab-on-ground is best idealized as a dense liquid. According to Pickett et al. (1951), the soil or subgrade beneath a slab behaves more like an elastic solid than a dense liquid. This is evident in the illustration from Hammons and Ioannides (1996) which shows the difference in behavior between a Winkler foundation and an elastic solid foundation, Figure 3-3. In a paper published in the Kansas State Engineering Experiment Station Bulletin, Pickett, Raville, Janes, and McCormick (1951) note

the limitations in Westergaard's theory from 1939 and prior. Pickett et al. pointed out that the Westergaard equations were restricted in that they did not account for multi-wheel landing gear on airplanes. In addition to the restrictions, Pickett et al. (1951) proposed their own corner loading stress equation, Equation 3-13, that was meant to replace Westergaard's. Additionally, Pickett et al. determined that the subgrade under slabs-on-ground behaves theoretically more like a deep elastic solid rather than a dense liquid as originally proposed by Westergaard. Research shows, however, that while the dense liquid subgrade idealization assumes that the deflection at points outside the loading area is equal to zero, resulting in lower stresses, Westergaard may have adjusted for these lower stresses in his equations through increasing the value used for the subgrade modulus of reaction in zones near the edge (Ioannides et al., 1985). Pickett et al. (1951) agreed that while the elastic solid subgrade theory may be a better approximation of actual subgrade behavior, the dense liquid theory was also worth consideration. This is evident in the creation of influence charts for both subgrade idealizations.

Stress Equation for Corner Loading Condition (Circular Load Area):

$$\sigma_{corner} = \frac{4.2P}{t^2}[1 - \frac{\sqrt{(a/l)}}{0.925 + 0.22(\frac{a}{l})}] \quad (3\text{-}13)$$

Following the work of Pickett, Raville, Janes, and McCormick, Pickett and Ray (1951) published a paper titled "Influence Charts for Concrete Pavements". Pickett and Ray developed these influence charts for the purpose of obtaining the moments and deflections in slabs-on-ground for interior and edge-loading conditions. While antiquated for today's computation technology, the influence charts worked by completing the following steps as outlined by Pickett and Ray (1951):

- On transparent paper, draw the area of the tires that are in contact with the slab in accordance with the properties of the slab and its supporting subgrade.
- Place the transparent paper on top of a blank influence chart in a position dependent on the location of the load with respect to the point for which a value for deflection or moment is desired.
- Count the number of blocks (positive or negative) that are covered by the tire areas.
- The number of blocks is then multiplied by the intensity of load and a factor dependent on slab and subgrade properties to obtain the desired value.

It is important to note that Poisson's ratio for concrete is assumed to have a value of 0.15 for all influence charts (Pickett and Ray, 1951). Figures 3-8 and 3-9 are used to calculate the deflection according to the above steps for an interior-loading scenario for the assumption of either a dense liquid subgrade or elastic solid subgrade. The deflection is calculated using Equation 3-14, where N represents the number of blocks covered by the wheel areas, P is the load intensity, and l represents the radius of relative stiffness. Redefined by Pickett and Ray (1951), the radius of relative stiffness is stated as a function of D, the flexural rigidity of the slab and C, the rigidity of the solid subgrade in order to relate dense liquid and elastic solid subgrade behavior in terms of a single variable. These are defined in Equations 3-15 through 18. Equation 3-16 is the same as Equation 3-4. It is repeated here for clarity in differentiating between Equation 3-16 and 3-17. The radius of relative stiffness for a dense liquid and elastic solid subgrade is calculated using Equations 3-16 and 3-17, respectively.

$$\text{Deflection, } \delta_{interior} = 0.0005\frac{Pl^4N}{D} \tag{3-14}$$

$$D = \frac{Et^3}{12\left(1-\nu^2\right)} \tag{3-15}$$

$$l = \sqrt[4]{\frac{D}{k}} = \sqrt[4]{\frac{Et^3}{12\left(1-\nu^2\right)k}} \text{ for a dense liquid subgrade} \tag{3-16}$$

$$l = \sqrt[3]{\frac{2D}{C}} = \sqrt[3]{\frac{t^3}{6}} \text{ for an elastic solid subgrade} \tag{3-17}$$

$$C = \frac{E}{\left(1-\nu^2\right)} \tag{3-18}$$

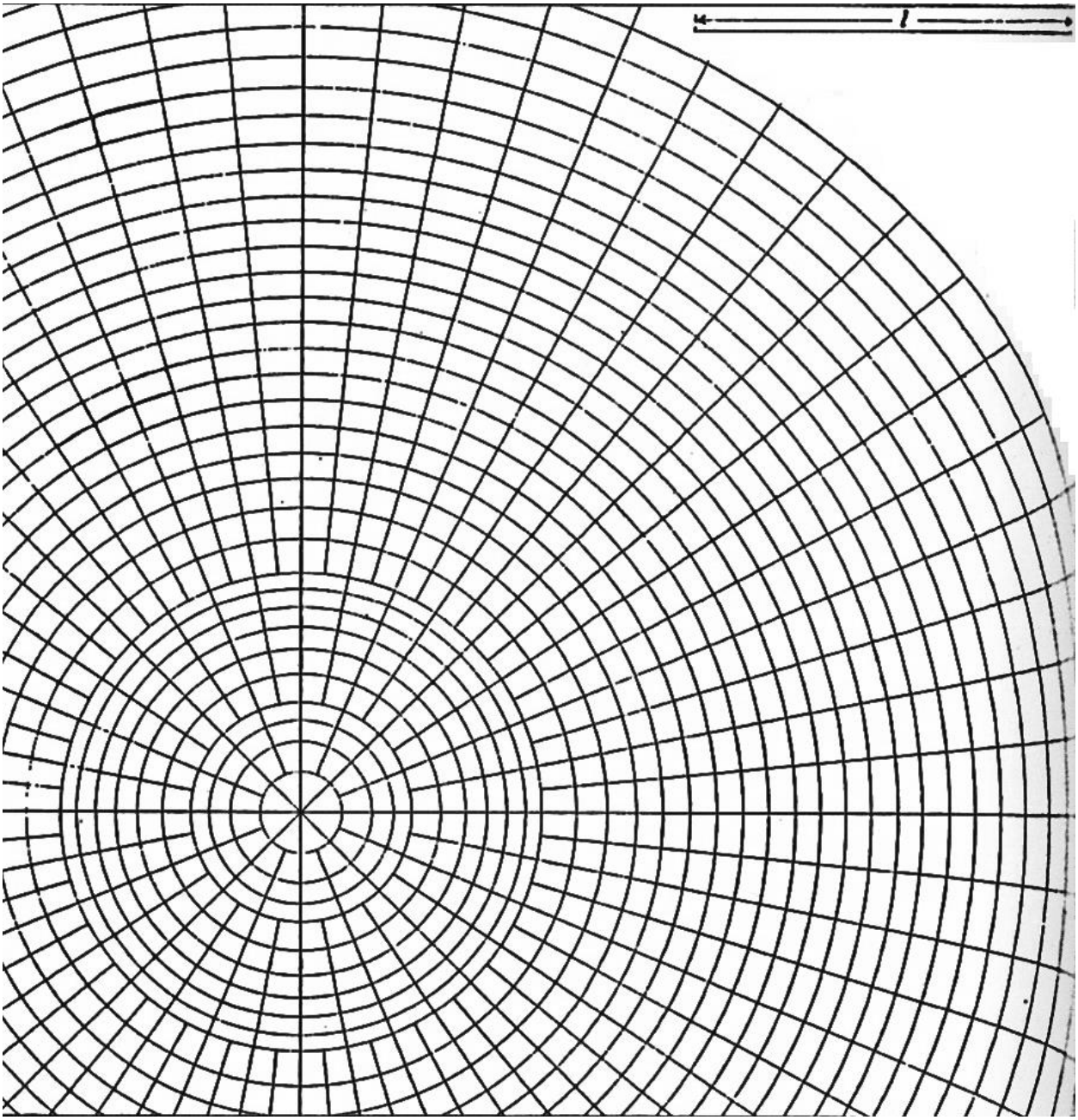

Figure 3-8: Influence Chart for the Determination of Deflection under Interior-Loading Assuming Dense Liquid Subgrade Behavior (Pickett and Ray, 1951)

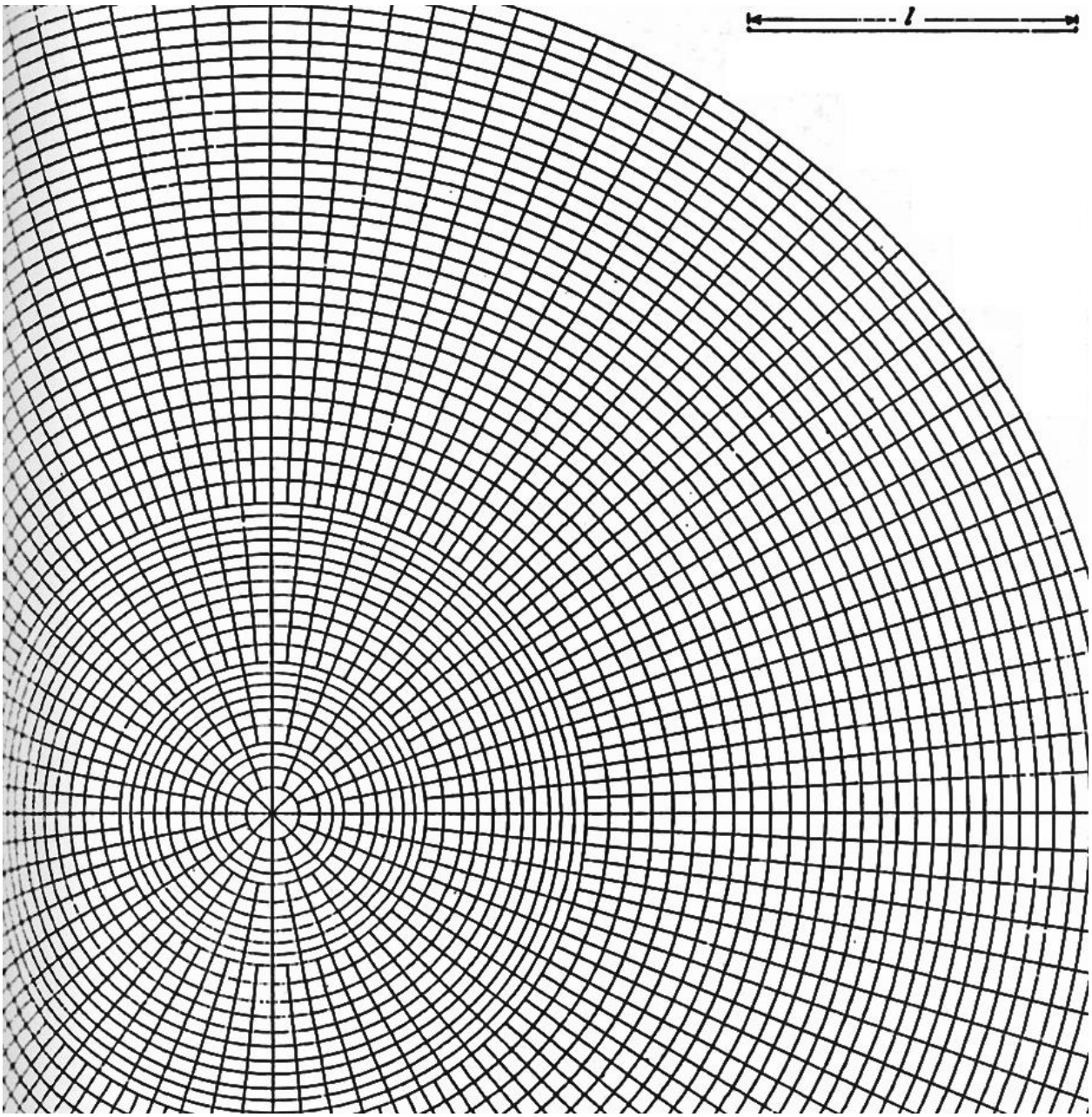

Figure 3-9: Influence Chart for the Determination of Deflection under Interior-Loading Assuming Elastic Solid Subgrade Behavior (Pickett and Ray, 1951)

The influence charts shown in Figures 3-10 and 3-11 are used for the calculation of slab deflections under edge loading conditions in addition to the deflections under a loading a

distance 0.5 times the radius of relative stiffness, l, from the edge; the latter of which is not considered by Westergaard.

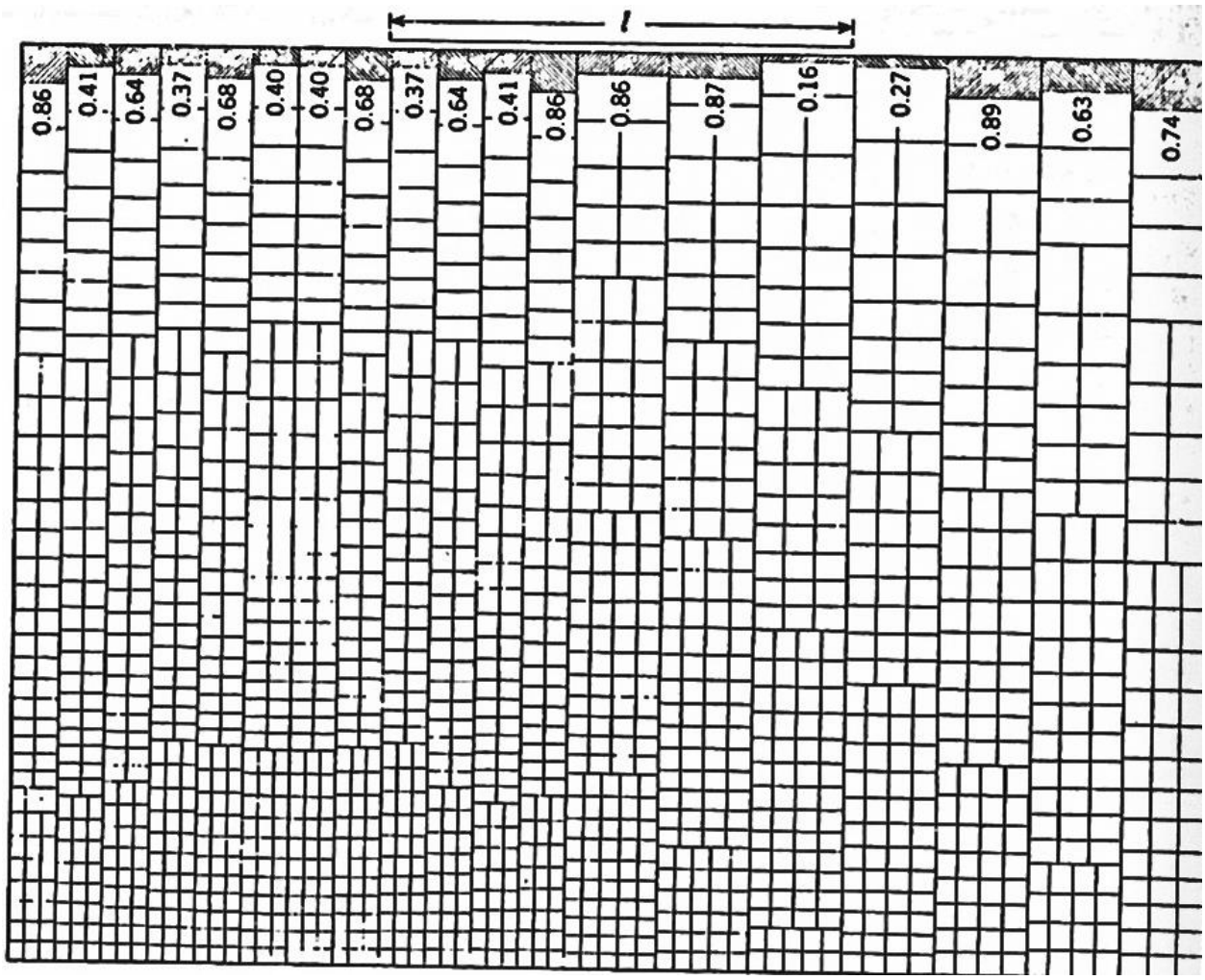

Figure 3-10: Influence Chart for the Determination of Deflection under Edge-Loading Assuming Dense Liquid Subgrade Behavior (Pickett and Ray, 1951)

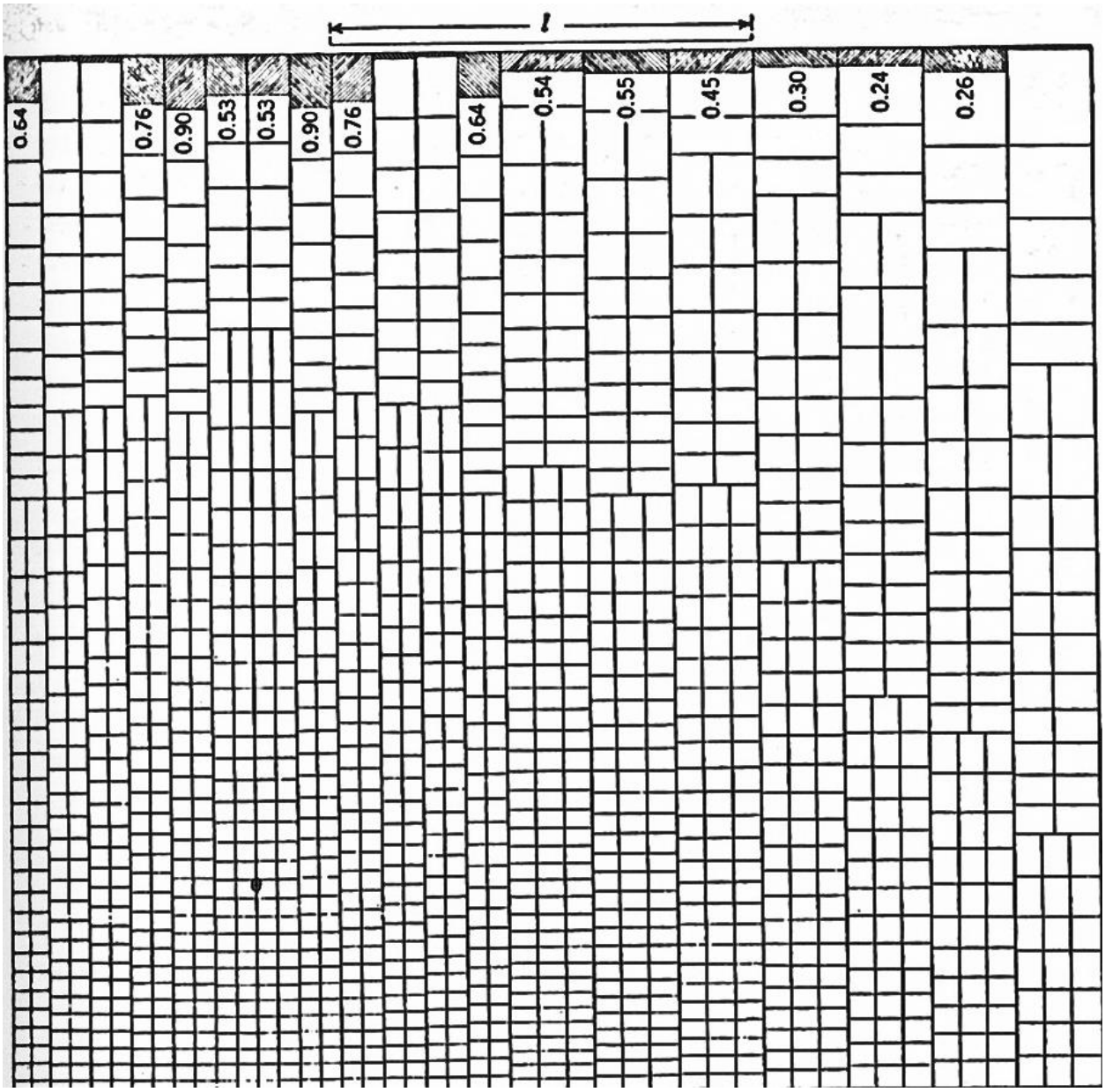

Figure 3-11: Influence Chart for the Determination of Deflection under a Load $0.5l$ from the Edge Assuming Dense Liquid Subgrade Behavior (Pickett and Ray, 1951)

Figures 3-12 and 3-13 depict the influence charts for determining the moment under interior loading assuming either dense liquid subgrade behavior or elastic solid subgrade behavior, respectively. The moment is calculated using Equation 3-19. The variables in Equation 3-19 have been previously defined above.

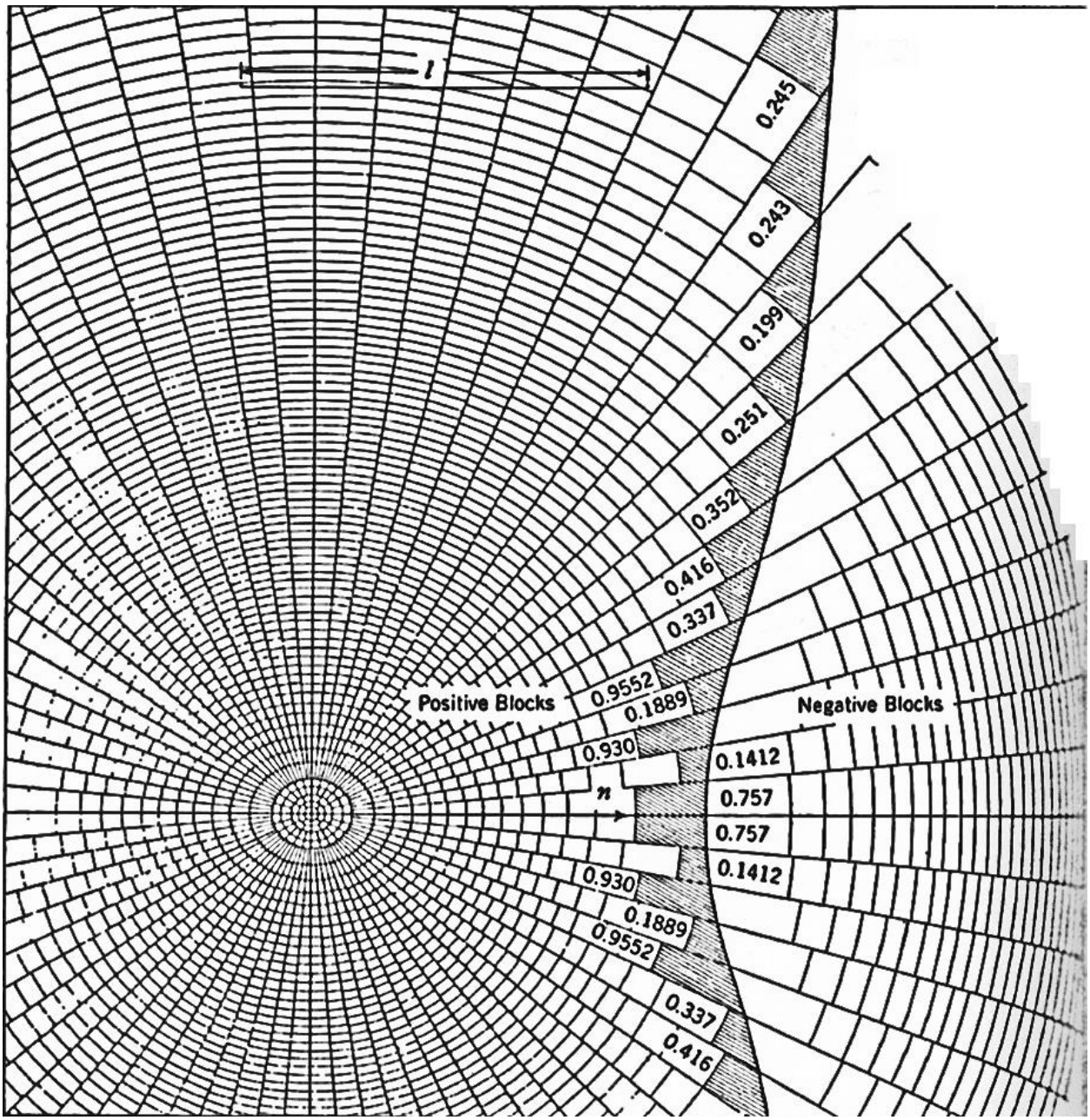

Figure 3-12: Influence Chart for the Determination of Moment under Interior-Loading Assuming Dense Liquid Subgrade Behavior (Pickett and Ray, 1951)

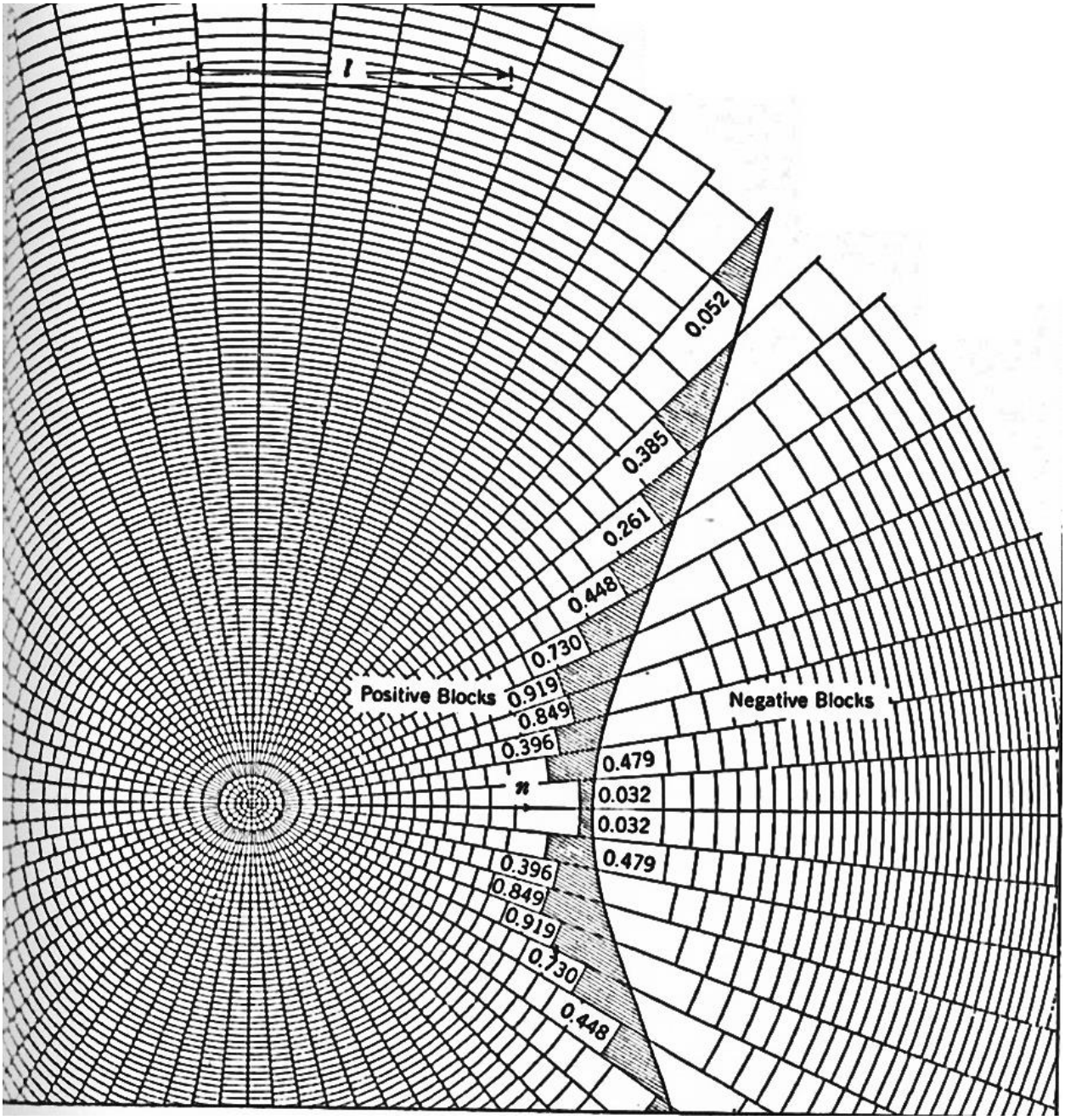

Figure 3-13: Influence Chart for the Determination of Moment under Interior-Loading Assuming Elastic Solid Subgrade Behavior (Pickett and Ray, 1951)

$$\text{Moment, } M = \frac{Pl^2 N}{10,000} \tag{3-19}$$

Figures 3-14 and 3-15 depict the influence charts for determining the moment under edge loading conditions in addition to the deflections under a loading a distance of $0.5l$ from the edge. Both assume dense liquid behavior.

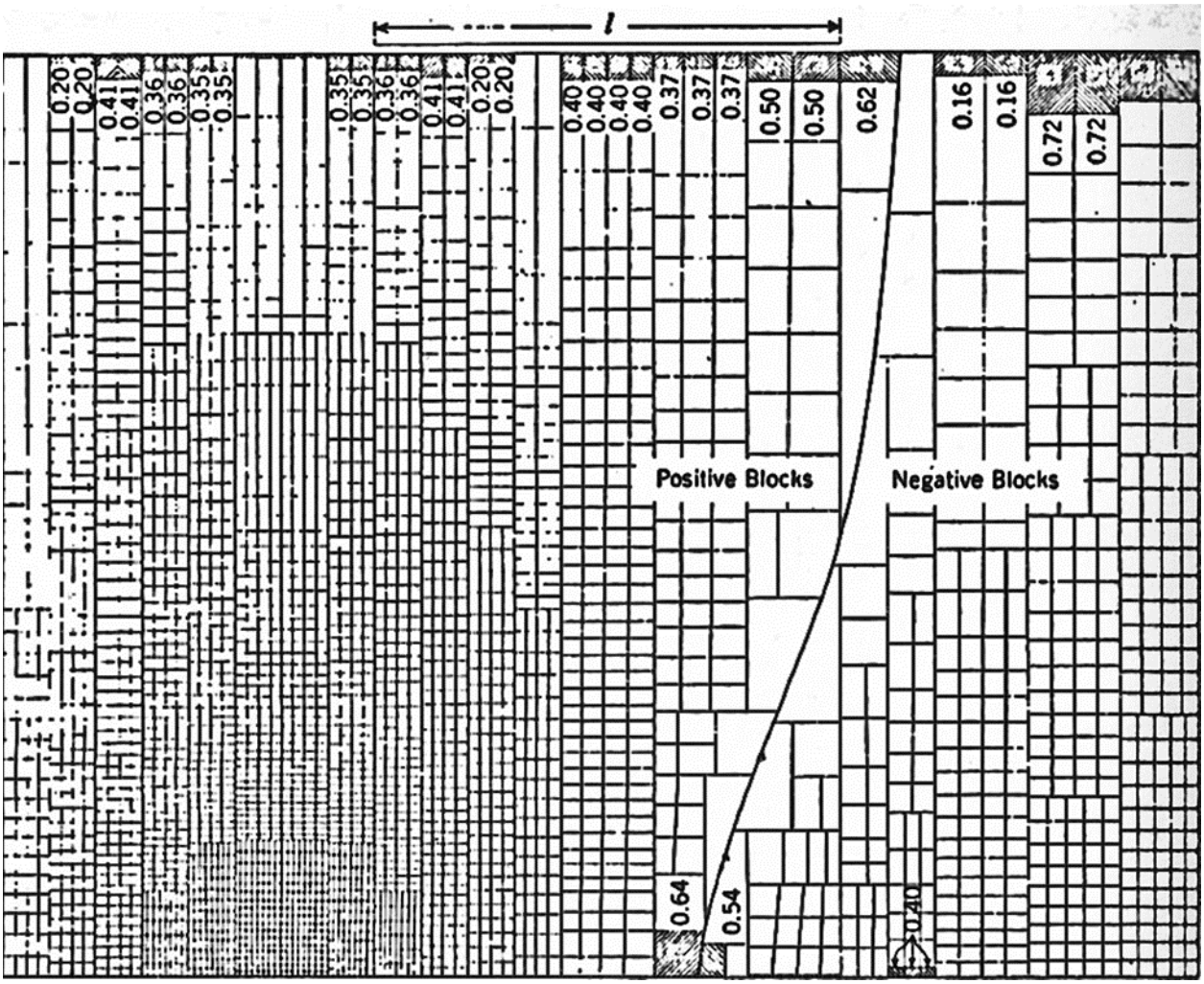

Figure 3-14: Influence Chart for the Determination of Deflection under Edge-Loading Assuming Dense Liquid Subgrade Behavior (Pickett and Ray, 1951)

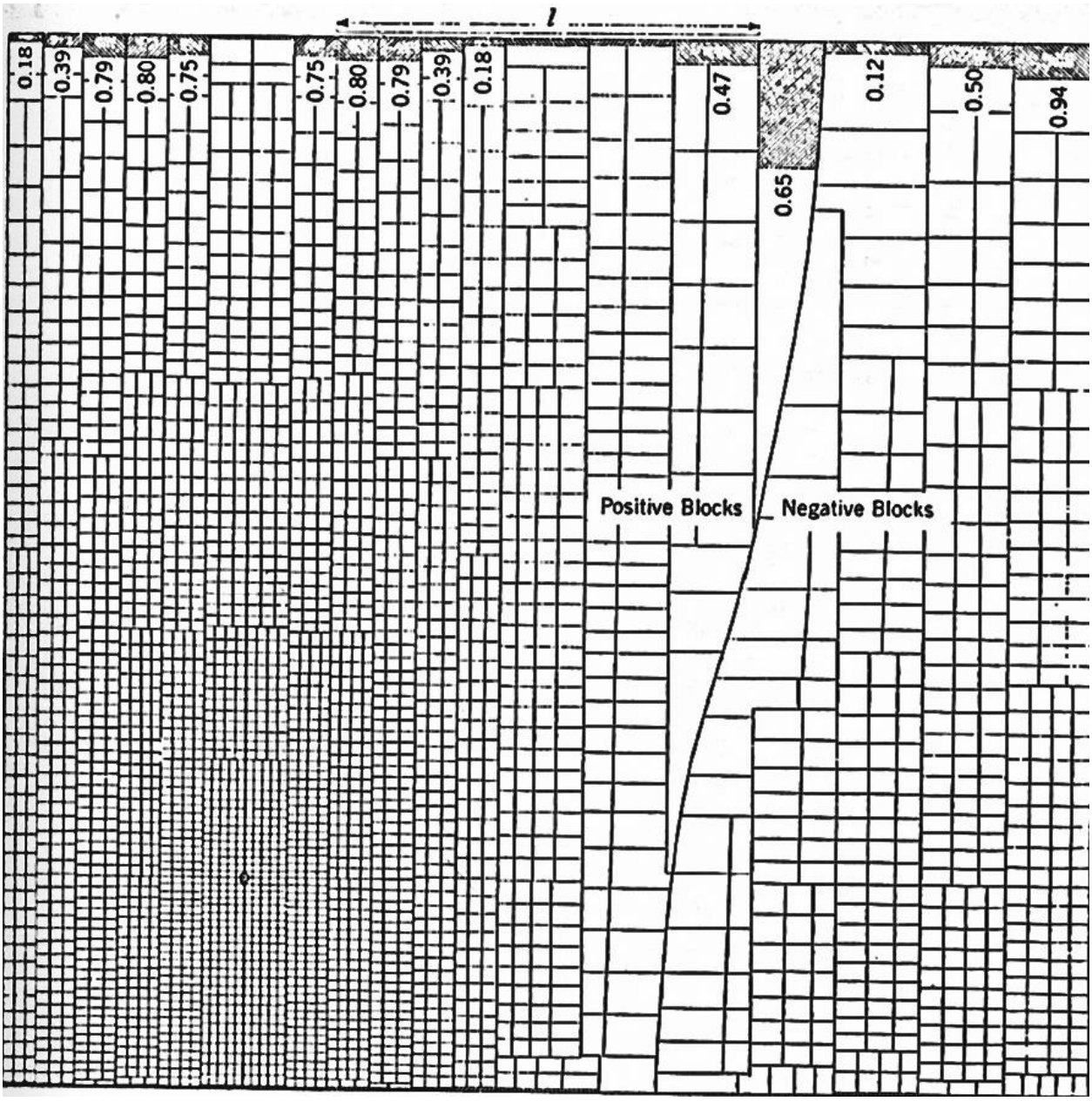

Figure 3-15: Influence Chart for the Determination of Moment under a Load $0.5l$ from the Edge Assuming Dense Liquid Subgrade Behavior (Pickett and Ray, 1951)

3.2.5 IOANNIDES, THOMPSON, BARENBERG, AND DONNELLY

A. M. Ioannides, Dr. M. R. Thompson, Dr. E. J. Barenberg, and J. Donnelly, under the management of Lieutenant Colonel Lawrence D. Hokanson, published a dissertation in 1984

titled *Analysis of Slabs-on-Grade for a Variety of Loading and Support Conditions* that considered many research tasks surrounding slabs-on-grade, finite element analysis, and Westergaard theory. Most importantly to this thesis, Ioannides et al. (1984) provided updates to Westergaard's original stress and deflection equations for the interior loading condition. This included improvements based on theoretical calculations and solutions to typographical errors. The equations for the equivalent radius, b, and the radius of relative stiffness, l, remained the same.

Prior to the work of Ioannides et al. (1985), A. M. Tabatabaie, E. J. Barenberg, and R.E. Smith (1979) published a report on the theoretical methods behind the use of ILLI-SLAB software. The software was used for computerized slab analyses. Tabatabaie et al. (1979) provided Equations 3-20 through 3-24 as the theoretical Westergaard equations used for the interior loading condition within the ILLI-SLAB software code. These vary slightly from the original Westergaard equations presented in Section 3.2.3. The changes in the equations were based on research conducted by Tabatabaie et al. (1979). As pointed out by Ioannides et al. (1985), the stress and deflection results do not differ much from results using Westergaard's original stress and deflection equations for the interior loading condition, but that the corner and edge loading condition results varied greatly.

Ioannides et al. (1984) provided yet another set of equations for the interior loading condition for the purpose of thoroughness. The "Ioannides equations" are more general, rigorous, and include "supplementary" stress first presented by Westergaard in 1939, which provided more specialized stress equations for airfield slab and pavement design applications (Westergaard, 1939). The more general equations are presented in Equations 3-25 and 26.

Stress Equation for the Interior Loading Condition (Tabatabaie et al., 1979):

$$\sigma_{interior} = \frac{0.275(1+\nu)P}{t^2}\left(4\log_{10}\left(\frac{l}{b}\right)+1.069\right) \tag{3-20}$$

Ordinary Theory:

$$b = a \text{ when } a \geq 1.724t \tag{3-21}$$

Special Theory:

$$b = \sqrt{1.6a^2 + t^2} - 0.675t \text{ when } a < 1.724t \tag{3-22}$$

Deflection Equation for the Interior Loading Condition (Tabatabaie et al., 1979):

$$\delta_{interior} = \frac{P}{8kl^2}\left[1-\frac{a^2}{l^2}\left(0.217-0.367\log_{10}\left(\frac{a}{l}\right)\right)\right] \tag{3-23}$$

$$l = \sqrt[4]{\frac{Et^3}{12(1-\nu^2)k}} \tag{3-24}$$

Stress Equation for the Interior Loading Condition (Ioannides et al., 1985):

$$\sigma_{interior} = \frac{3(1+\nu)P}{2\pi t^2}\left[\ln\left(\frac{2l}{a}\right)-\gamma+\frac{1}{2}+\frac{\pi}{32}\left(\frac{a}{l}\right)^2\right] \tag{3-25}$$

Deflection Equation for the Interior Loading Condition (Ioannides et al., 1985):

$$\delta_{interior} = \frac{P}{8kl^2}\left[1+\frac{1}{2\pi}\left(\ln\left(\frac{a}{2l}\right)+\gamma-\frac{5}{4}\right)\left(\frac{a}{l}\right)^2\right] \tag{3-26}$$

Where Euler's Constant, γ = 0.57721566490153286061

3.3 FROM THEORY TO PRACTICE

Ioannides et al. (1984) assert that several of the design codes reference the original Westergaard equations without explicitly listing the equations themselves. The design codes

also consider multi-wheel loading conditions, which, as described, are not included in Westergaard's equations. For these reasons, there is an indication that the design charts are based on the influence charts from Pickett and Ray (1951) and the governing differential equations used to create those influence charts. That being said, the Pickett and Ray influence charts are, in fact, based on a modified version of Westergaard theory so, in a way, the design guides are based on Westergaard theory, but not pure Westergaard theory. The following sections provide a more specific description on the origin of each design guide.

The increasing prevalence of Westergaard's equations and all the research conducted alongside and after him led to the need for a design manual in which these design procedures were summarized. Rice, Eberhardt, and Varga (1974) prepared a technical manual for the design of concrete slabs-on-ground subjected to heavy loads. According to Rice et al. (1974), the manual was developed by re-examination and revision to existing design procedures based on field surveys of the type and volume of vehicular traffic. In the early 2000's, the technical manuals (TMs) of each branch of the military were combined into the UFC in order to create a more unified approach to design and analysis. The most relevant UFC to this research is UFC 3-320-06A: Concrete Floor Slabs on Grade Subjected to Heavy Loads.

CHAPTER 4: NUMERICAL INVESTIGATION INTO THE ORIGINS AND FACTORS OF SAFETY OF VARIOUS SLAB THICKNESS SELECTION METHODS

4.1 CALCULATION SET-UP

There is a lack of published information that can be used to draw a precise and numerical connection between Westergaard theory and the design specifications and guides used in today's practice of designing and analyzing slabs-on-ground. However, we know that there is, in fact, a connection to Westergaard's work based on references cited in various design guides. ACI 360R, for example, explicitly cites Westergaard as their basis for stress calculations. For these reasons, the calculations within this chapter were conducted in order to infer a connection between the design charts and nomographs of each slab-on-ground thickness selection method and the Westergaard equations. Furthermore, calculations were conducted to establish relationships between how variables and assumptions such as the loading area, the load itself, the modulus of subgrade reaction, and Poisson's ratio affect Westergaard stress results.

This section of this thesis provides a connection based on a couple of different comparisons. These comparisons include an analysis of slab-on-ground design thickness results determined using four different methodologies and a comparison to the Westergaard theory stress results. From the Westergaard analysis, an attempt was made to extract any factors of safety, if any, built-into the charts and nomographs of the PCA, ACI 360R, UFC, and COE methods as described in the following paragraph.

Based on guidance from *Designing Floor Slabs on Grade* by Boyd C. Ringo and Robert B. Anderson (1996), calculations were conducted to design a slab-on-ground by four different methods in order to make a comparison and contrast between them. These four methods include the COE method, the UFC method, the PCA method, and the ACI 360R method, the last of which is not included in the Ringo and Anderson text. Nevertheless, ACI 360R is included in this research because it is concerned with the design of slabs-on-ground and makes use of the direct application of Westergaard's equations for the purpose of slab-on-ground thickness selection. Ringo and Anderson (1996) report six different methods for designing slabs-on-ground, but this research focused on the four above-mentioned methods as they are the most relevant in the design of slabs-on-ground in hangar foundation applications.

The four methods from Ringo and Anderson's book that were excluded from this research include the Wire Reinforcement Institute (WRI) method, the Post-Tensioning Institute (PTI) method, the ACI Committee 223 (ACI 223) method, and the Finite Element Analysis method. The WRI method was excluded because it is so similar to the PCA method. Engineers at the Air Force Civil Engineer Center more-often use the PCA method, so it was used in this research. The PTI method was excluded from this research because it is used for the design of slabs-on-ground that are post-tensioned. For the sake of a clean comparison, no post-tensioned slabs-on-ground were considered. The ACI 223 method was not included in this research because it does not deal directly with the selection of slab thickness, which must be calculated using another method referenced within the ACI 223 document (Ringo and Anderson, 1996). Finally, the Finite Element Analysis method of slab-on-ground thickness selection was not considered in this research because it a computer-based method and this research focuses on slab

thickness calculations by using design charts and nomographs. Before using the design charts and nomographs, some initial information was required.

In this research, initial inputs for slab designs were selected based on a specific military aircraft because of its common use within the United States DoD. According to Ringo and Anderson (1996), the designer must select the factor of safety to apply to the stresses such as the maximum tensile stress that is set equal to the modulus of rupture prior to using the design charts and nomographs. Ringo and Anderson (1996) recommend using a factor of safety between 1.7 and 2.0. The requirement of selecting a factor of safety to apply prior to using the nomograph or chart in each method indicates that there are not likely any factors of safety already built into them. This was a major question posed by the Air Force Civil Engineer Center. For these computations, no factor of safety was applied prior to use of the design charts and nomographs for the purpose of making a direct comparison between the four methodologies and for direct comparison with Westergaard stress analysis results.

The modulus of rupture was estimated using Equation 4-1. Ringo and Anderson's computations utilized a modulus of rupture equal to nine times the square root of the compressive strength of the concrete. A value of seven and a half times the square root of the compressive strength of the concrete is used in this research because it is a more conservative estimate. The concrete compressive strength, f'_c, must be input into Equation 4-1 in units of pounds per square inch (psi).

$$f_r = 7.5\sqrt{f'_c} \tag{4-1}$$

*Note: value for f'_c must be in units of psi

Using initial values for the concrete compressive strength, the modulus of rupture, the subgrade modulus k , and the loading condition, results for the selected slab thicknesses were reported for each of the four methods as shown in Section 4.5.

Table 4-2 summarizes the initial inputs reflect Lockheed Martin's F-16 Fighting Falcon specifications. This aircraft is one of many commonly used by The United States Air Force as depicted in Figures 4-1 and 4-2. Denoted on Figure 4-2, the main body tires are the two tires towards the wings of the aircraft and the nose tire is the single tire centered towards the nose of the aircraft. According to Michelin's Military Brochure (Michelin, 2015), for an F-16 model C or D aircraft, the nose and main body tire sizes are 18X5.7-8 and 27.75X8.75-14.5, respectively. Three-part tire sizes like these denote the overall diameter of tire, the width of the tire, and the diameter of the wheel as shown in Table 4-1.

Figure 4-1: Nose View of an F-16 Fighting Falcon at Misawa Air Base in Japan (Barnett, 2008)

Figure 4-2: Side View of an F-16 Fighting Falcon at Misawa Air Base in Japan (Barnett, 2008)

Table 4-1: Tire Size Labels Defined

Wheel	Tire Size	Overall Diameter (in)	Tire Width (in)	Wheel Diameter (in)
Nose Wheel	18X5.7-8	18	5.7	8
Body Wheels	27.75X8.75-14.5	27.75	8.75	14.5

The load contact area, A, was calculated using an approximation by Mellgren (1980) as shown in Figure 4-3. The overall radius of the tire and the wheel, R, is multiplied by the width of the tire, b. These values are found in Table 4-2.

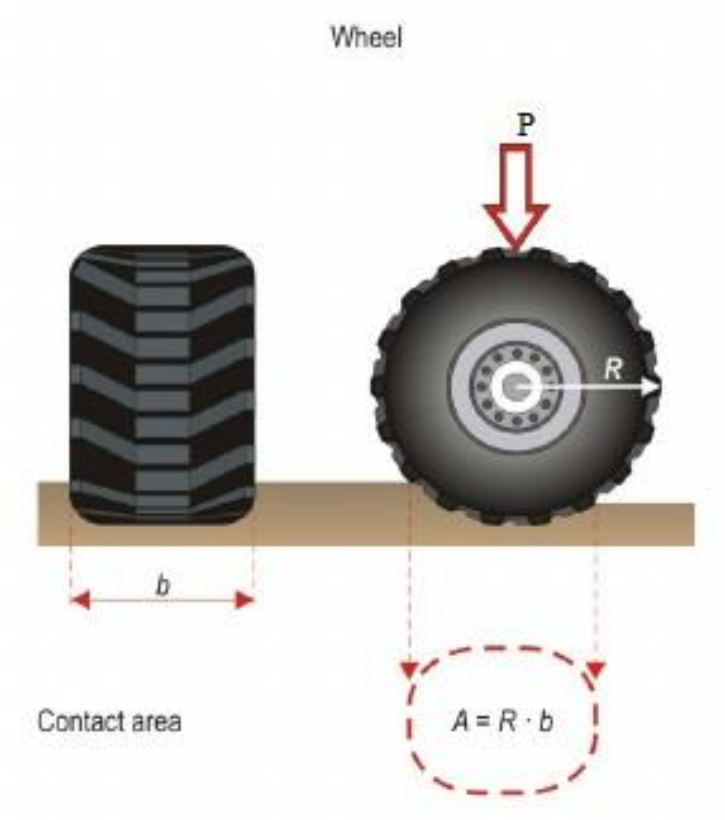

Figure 4-3: Theoretical Set-up for Calculation of Wheel Load Area (Mellgren, 1980)

Table 4-2: Initial Inputs for Computations

F-16 Fighting Falcon		
Aircraft Specifications		
Maximum Aircraft Weight at Takeoff (lbs)		48000
Number of Wheels		Three
Type of Tires (Solid or Pneumatic)		Pneumatic
Typical Aircraft Tire Pressure (psi)		320
Spacing between Body Wheels (in)		93.5
Spacing between Body and Nose Wheels (in)		158
	Nose Wheel	**Body Wheels**
Width of Wheel, b (in)	5.70	8.75
Radius of Unloaded Wheel, R (in)	9.00	13.88
Wheel Contact Area, A (in^2)	51.30	121.41
Site and Material Specifications		
Concrete Compressive Strength, f'_c (psi)		4000
Concrete Modulus of Rupture, f_r (psi)		474
Modulus of Subgrade Reaction, k (pci)		200

The load, P, for stress analysis purposes was assumed to be equal to the maximum aircraft weight at takeoff of 48,000 pounds (Lockheed Martin, 2018). This value was selected to be the worst-case scenario loading since this is the largest total weight that this particular aircraft is permitted to weigh including fuel, cargo, and passengers. All aircraft have three tire assemblies, or gears, either single or dual axle, which distribute the weight of the aircraft into the slab. The "main gear", which correspond to the tire assembly under the main body support about 95% to 98% of the aircraft's entire weight. The "nose gear" supports the remaining 2% to 5% of the aircraft's weight. In this case, each tire is loaded to 320 pounds per square inch. This value

can be used to estimate the contact area of the load by dividing the load per wheel by the tire pressure (Ringo and Anderson, 1996), however, it is more precise to use manufacturer specifications and the procedure shown in Figure 4-3. The latter method was used in these calculations and the results are shown in Table 4-2.

Typical values were selected for the concrete compressive strength, the concrete modulus of rupture, and the modulus of subgrade reaction. The concrete modulus of rupture f_r was calculated using Equation 4-1. There are many versions of this equation to estimate the modulus of rupture, but in this case a multiplier of 7.5 was used as a conservative estimation.

The spacing between the three tires was specified as shown in Figure 4-4. The center of gravity of the F-16 Fighting Falcon is a distance past the body tires that is approximately ten percent of the spacing from the body tires to the nose tire. In this case, the center of gravity (c.o.g.) is located 15.8 inches forward of the body tires.

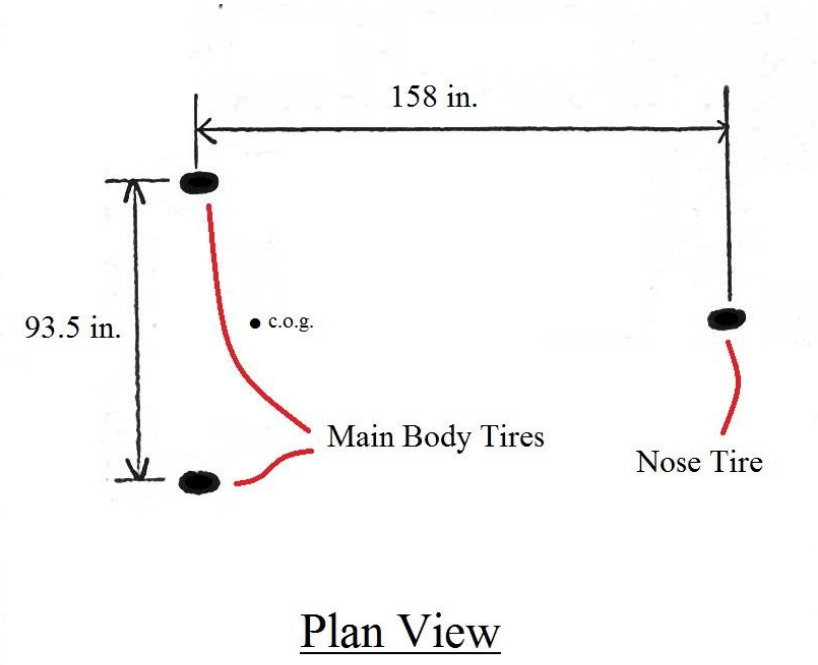

Figure 4-4: Plan View of Wheel Spacing of F-16 Fighting Falcon

4.2 SLAB-ON-GROUND THICKNESS SELECTION USING THE PCA METHOD RESULTS AND DISCUSSION

Using the calculation set-up from Section 4.1, the stress per wheel load, measured in pounds per square inch, was calculated for use in the PCA design chart. The Portland Cement Association (1955) explicitly states that a factor of safety is not built into the design chart. The recommended safety factors are shown in Table 4-3. The modulus of rupture value computed in Section 4.1 was used as the flexural strength for use in the UFC and COE design charts. The modulus of rupture, in psi, was divided by the total axle load in the body wheels, in kips, to get a value of 10.98 psi for the stress per 1000-pound axle load required for input into the charts. Based on the location of the center of gravity as described in Section 4.1, the body wheels were determined to carry 21,600 pounds of aircraft load per tire and the nose tire was determined to carry 4,800 pounds of aircraft load (Table 4-3). These calculations are shown in Equations 4-2 and 4-3 using the set-up shown in Figure 4-5. When calculating the moments in the slab, counter clockwise was assumed positive. The upwards direction was assumed to be positive for the calculation of shear in the slab.

Table 4-3: Recommended Safety Factors (PCA, 1955)

Installation	**Safety Factor**
Aprons, taxiways, hard standings, runway ends, **hangar floors**	1.7 - 2.0
Runways (central portion)	1.25 - 1.5

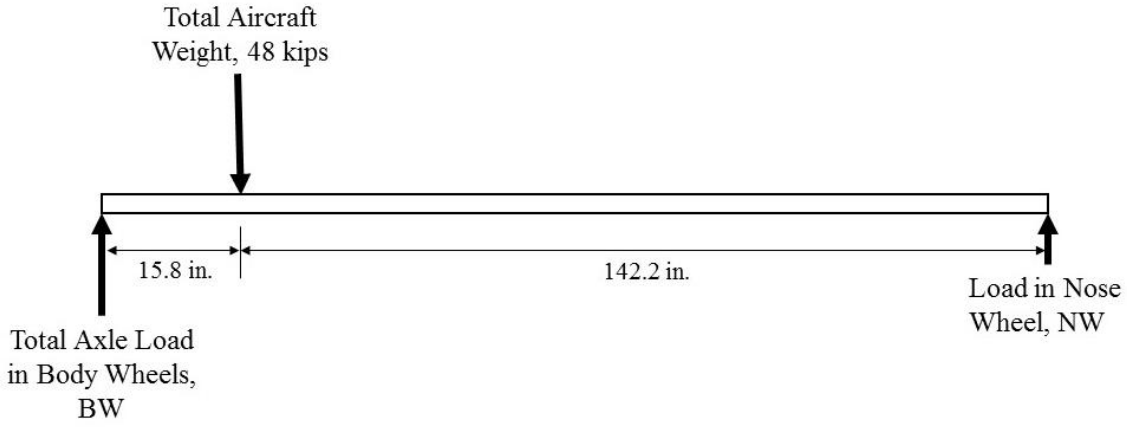

Figure 4-5: Free Body Diagram for Calculations in Equations 4-2 and 4-3

$$CCW(+), \sum M_{BW} = -48kips(15.8in) + NW(158in) = 0$$
$$\therefore NW = 4.8kips \quad (4\text{-}2)$$

$$\uparrow (+), \sum V = BW - 48kips + 4.8kips = 0$$
$$\therefore BW = 43.2kips \quad (4\text{-}3)$$

Table 4-4: Body Wheel Loading

Load in each Body Wheel (kips)	21.6
Total Axle Load (kips)	43.2
Stress per 1000 lb. Axle Load (psi)	10.98

The Portland Cement Association method for slab thickness selection is based on the influence charts created by Pickett et al. (1951) (Ringo, 1986). ACI 360R references several methods for selecting slab-on-ground thickness including the use of the PCA method. ACI 360R describes the PCA design chart as only considering loads applied to the interior of the slab-on-ground (ACI 360R, 2010). Using the PCA design chart, in Figure 4-6, and the input values computed in Section 4.1 for the body wheels, a slab thickness of seven inches was calculated.

No factor of safety was used in this computation because it was used to compare with Westergaard stress computation results. The dashed line in Figure 4-6 represents the example in the design guide; the red line in the figure represents actual results from this design example. The slab thickness was determined by starting at the y-axis (left side of chart) and drawing a horizontal line from the computed stress per 1000 pounds of total body wheel axle load (calculated using Equation 4-4) to the effective contact area, which was approximately 121.41 square inches for the body tires. Next, a vertical line was drawn from the effective contact area to the wheel spacing of 93.5 inches. Finally, a horizontal line was drawn from the wheel spacing to the subgrade modulus, which was assumed to be 200 pounds per cubic inch. This resulted in a slab thickness of seven inches as shown in Table 4-5.

Stress per 1000-Pound Axle Load, $\frac{f_r}{BW} = \frac{474\,psi}{43.2\,kips} = 10.98\,psi$ (4-4)

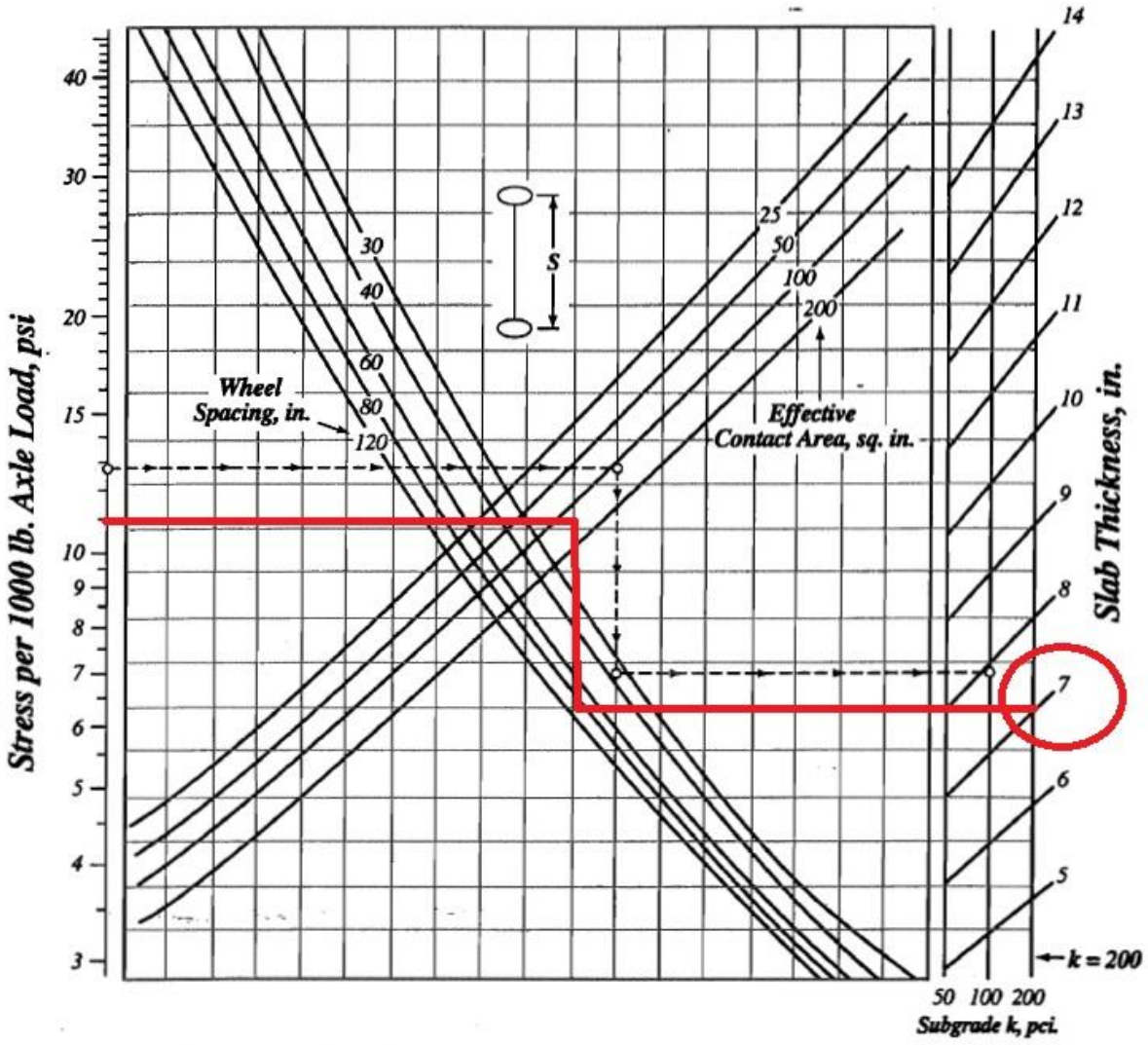

Figure 4-6: Results for Slab Thickness Using the PCA Design Chart

Table 4-5: Slab Thickness Results using the PCA Method

PCA Method	
Load in Each Body Wheel (kips)	21.6
Total Axle Load (kips)	43.2
Stress per 1000 lb. Axle Load (psi)	10.98
Modulus of Subgrade Reaction, k (pci)	200.00
Slab Thickness (in)	7

4.3 SLAB-ON-GROUND THICKNESS SELECTION USING THE UFC AND COE METHODS RESULTS AND DISCUSSION

Results for slab thickness were also selected using the design chart that appears in UFC 3-320-06A, which is the same design chart originally presented by the Corps of Engineers. This design slab thickness method only considers loads applied to the edges of a slab-on-ground (ACI 360R, 2010). The initial inputs required for using the UFC/COE design chart include the flexural strength of the concrete, the modulus of subgrade reaction k, and the design index. The modulus of rupture of the slab-on-ground for the F-16 Fighting Falcon was computed in Section 4.1 and is equal to 474 pounds per square inch. This value was taken as the flexural tensile strength for use in the UFC design chart. The same value for the modulus of subgrade reaction of 200 pounds per cubic inch, as used in the PCA design example, was used in the UFC design chart for comparison purposes.

The final value needed in the design chart is the design index (DI). The DI is defined as a value that describes the relative severity of slab-on-ground loading based on varying axle loadings and traffic volume described by a maximum number of operations or passes per day over a span of 25 years (UFC 3-320-06a, 2005). The difference between the design charts in UFC 3-320-06a and the Corps of Engineers Design Manual for Concrete Floor Slabs-on-Grade is simply the design index selection criteria, with the more up-to-date criteria from the UFC guide being more conservative. Though a description of the DI is given in the UFC 3-320-06a manual, no clear and specific information is given on selecting a DI. A design index of 5 was selected based on guidance from ACI 360R-10, which references the COE method, summarized in Table 4-6 showing the criteria for design index categories one through six. Table 4-6 does not appear to take into account the traffic volume defined in the UFC description of the design index.

Nevertheless, the F-16 aircraft identifies best with a DI of 5 according to procedures laid out by the ACI 360 method.

Using the flexural strength, the modulus of subgrade reaction, and the DI, a value for slab thickness was found to be 7.1 inches. As in Figure 4-7, starting from the y-axis of flexural strength, a horizontal line was drawn from the flexural strength, equal to 474 psi, to the curve for the modulus of subgrade reaction k and then vertically to the line for a design index of 5. Finally, a horizontal line was drawn straight across to the design slab thickness. A summary of the UFC/COE method results are shown in Table 4-7.

Table 4-6: Criteria for Selection Design Index Category (ACI 360R, 2010)

Design Index Selection Criteria According to ACI 360						
Category	**I**	**II**	**III**	**IV**	**V**	**VI**
Design Axle Load (lb)	10000	15000	25000	36000	43000	120000
Type of Tire	Solid	Solid	Pneumatic	Pneumatic	Pneumatic	Pneumatic
Tire Contact Area (in^2)	27	36.1	62.5	100	119	316

*Note: This table was condensed from Appendix A of ACI 360R-10.

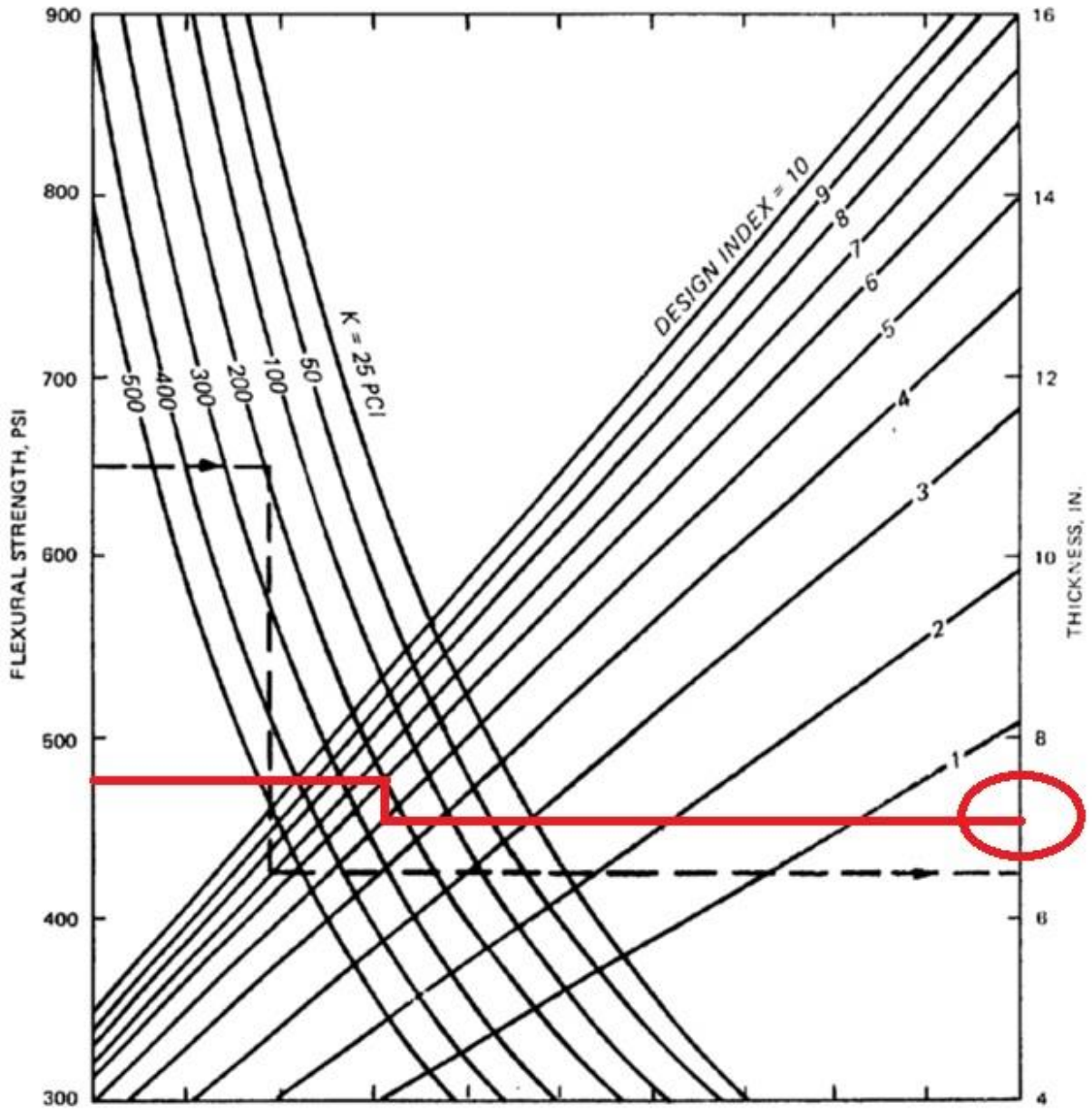

Figure 4-7: Design Slab Thickness Results using the UFC and COE Design Chart

Table 4-7: Design Slab Thickness Results using the UFC/COE Method

UFC 3-320-06A/COE Method	
Flexural Strength (psi)	474
Modulus of Subgrade Reaction, k (pci)	200
Design Index	5
Slab Thickness, t (in)	7.10

According to the ACI 360 manual (2010), the chart appearing in the COE and UFC methods is based on using an impact factor of 25%, a modulus of elasticity of the concrete of 4000 kips per square inch, and a factor of safety of 2. It is not clear, however, what role each of these play in calculating the slab thickness.

4.4 SLAB-ON-GROUND THICKNESS SELECTION USING THE ACI 360 METHOD RESULTS AND DISCUSSION

In the Westergaard stress analyses and the ACI 360 method, the semi-elliptical wheel contact areas needed to be converted to circular loading areas. An equivalent diameter, d_e, and equivalent radius, r_e, was calculated using the approach shown in Figure 4-8 (Engineering ToolBox, 2003). Results are summarized in Table 4-8.

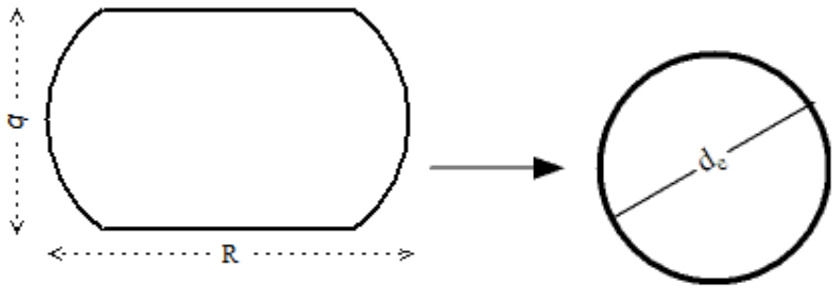

Figure 4-8: Calculation of an Equivalent Diameter (Engineering ToolBox, 2003)

Table 4-8: Equivalent Diameters and Radii for Body and Nose Wheels

Equivalent Lengths	**Body Wheels**	**Nose Wheel**
Equivalent Diameter, d_e (in)	11.46	7.45
Equivalent Radius, r_e (in)	5.73	3.73

The ACI 360R-10 design method describes steps to determine the design slab thickness depending on whether the slab-on-ground is unreinforced or reinforced. For purposes of comparison, only unreinforced slabs-on-ground were considered. The selection of design thickness for reinforced slabs-on-ground involves the use of the nomograph presented in Chapter 2. For slabs-on-ground that are unreinforced, ACI 360R-10 suggests several options for determining the design slab thickness. These include the direct application of the Westergaard equations, the PCA method, and the COE method. The latter two are already calculated and results are in this chapter's previous section.

Tables 4-9 and 4-10 show results for the direct application of the Westergaard equations. The values for the wheel load, the equivalent radius of the wheel loading area as calculated in Section 4.1, the modulus of subgrade reaction, and Poisson's ratio were input into Equations 3-8 and 3-11, Westergaard's stress equations for interior and edge loading. Both values were calculated in order to make a comparison between the ACI 360 method and the PCA and UFC/COE methods, which are based on either interior loading or edge loading, respectively. The value for the stress in the slab was selected to be equal to the modulus of rupture. Using these inputs, the result for the design slab thickness using the ACI method for unreinforced slabs-on-ground was 7.48 inches under the interior loading condition and 9.44 inches under the edge loading condition.

Table 4-9: ACI 360R Method Results for Design Slab Thickness Selection for Unreinforced Slabs-on-Ground using Westergaard Stress Equation for Interior Loading (ACI360R-10, 2010)

ACI Method (Interior-Loading)	
Load in each Body Wheel (kips)	21.6
Radius of Unloaded Wheel, a (in)	5.73
Modulus of Subgrade Reaction, k (pci)	200
Poisson's Ratio, ν	0.15
Slab Thickness, t (in)	7.48
Stress in Slab (psi)	474

Table 4-10: ACI 360R Method Results for Design Slab Thickness Selection for Unreinforced Slabs-on-Ground using Westergaard Stress Equation for Edge Loading (ACI360R-10, 2010)

ACI Method (Edge-Loading)	
Load in each Body Wheel (kips)	21.6
Radius of Unloaded Wheel, a (in)	5.73
Modulus of Subgrade Reaction, k (pci)	200
Poisson's Ratio, ν	0.15
Slab Thickness, t (in)	9.44
Stress in Slab (psi)	474

4.5 SUMMARY OF SLAB THICKNESS RESULTS AND COMPARISON OF SLAB-ON-GROUND THICKNESS SELECTION METHODS

The slab-on-ground design thickness results for each method are summarized in Table 4-11. There was good agreement between the thickness results for the PCA, UFC/COE, and the interior loading condition ACI 360R design methods. The slab thickness result using the ACI 360R design method for the edge loading condition was slightly higher than the aforementioned.

These results confirm several previously mentioned assertions. First, the results for slab thickness should be similar between the methods since they are all based on Westergaard's equations. The PCA and UFC/COE methods are applicable only to the interior and edge loading conditions, respectively; indeed, the PCA method results are in agreement with the corresponding ACI 360R results for interior loading. The same idea applies to the latter; the UFC/COE method results are also in agreement with the corresponding ACI 360R results for edge loading. Furthermore, this correspondence demonstrates the link between Westergaard's stress equations and the nomographs and design charts from the PCA and UFC/COE methods.

Table 4-11: Summary of Slab-on-Ground Design Thickness Results

Slab-on-Ground Design Thickness Selection Method	Design Slab Thickness Results (inches)
Portland Cement Association	7.00
Corps of Engineers/Unified Facilities Criteria	7.10
American Concrete Institute (Unreinforced, Interior Loading)	7.48
American Concrete Institute (Unreinforced, Edge Loading)	9.44

Using these results, a comparison was made between the two corresponding sets of data: interior loading and edge loading. This comparison was made based on previous findings that the PCA design chart is based on the Westergaard equations for the interior loading condition and the UFC/COE design chart is based on the Westergaard equations for the edge loading condition. The comparison allowed inferring that, most likely, there is a factor of safety of approximately 1.3 built into the UFC 3-320-06A/COE design chart as shown in Table 4-12. It is important to note, however, that this factor of safety changed depending on the design index selected. The ACI 360 manual (2010) asserts that the chart appearing in the COE and UFC methods is based on using an impact factor of 25%, a concrete modulus of elasticity of 4000 kips per square inch, and a factor of safety of 2. Since it is not clear what role each of these play in calculating the slab thickness, it was determined that the factor of safety in the UFC/COE design chart is somehow included in the form of a severity rating or design index rather than just a specific multiplier built into the chart. Other than the design index, there is no information within the UFC 3-320-06A design guide that provides an explanation of factors of safety

involved in the use of this design chart nor its origins. The only evident safety provision was assuming the flexural strength of the concrete to be equal to the modulus of rupture.

Research into the origins of the COE design chart for determining slab-on-ground thickness revealed that it is based only partly on Pickett and Ray's influence chart for the maximum stress in an edge-loading scenario (Eberhardt, 1973), which might explain a discrepancy between UFC/COE results and results from the direct application of Westergaard's edge-loading stress equation. Based on these findings, it was determined that the design index serves as a sort of factor of safety since it is not a variable in Westergaard's stress equations and is dependent on the severity of loading conditions.

Table 4-12: Built-in Factors of Safety Determined by Numerical Computations

	Ratio of Slab Thicknesses	**Possible Built-in Factor of Safety?**	**Factor of Safety**
PCA versus ACI 360 (Unreinforced, Interior Loading)	1.07	No	1.0
UFC/COE versus ACI 360 (Unreinforced, Edge Loading)	1.33	Yes	1.30

4.6 WESTERGAARD STRESS EQUATION NUMERICAL INVESTIGATION RESULTS AND DISCUSSION

Based on the use of the Westergaard equations presented in Section 3.2.3, the input values in Table 4-13 were selected in order to perform example calculations. Slab thickness, t, and the modulus of subgrade reaction, k, were varied in order to determine their effect on the stress in the slab-on-ground. Several slab thicknesses between 6 and 12 inches and subgrade

moduli between 50 and 200 were considered. The same concrete compressive strength and Poisson's ratio were used for this example calculation as used in the previous section calculations, resulting in the same modulus of elasticity of concrete and modulus of rupture. The modulus of elasticity of the concrete was estimated using Equation 4-5, where *w* represents the unit weight of normal weight plain concrete in pounds per cubic foot. The equation requires the compressive strength of the concrete to be entered in as pounds per square inch. The same radius of circular loading area of 5.73 inches of the body wheels and the load of 21,600 pounds were used. Table 4-14 shows the computation results for the radius of relative stiffness as well as the stress in the slab-on-ground for the corner, interior, and edge loading conditions.

$$E_c = 33w^{1.5}\sqrt{f'_c} = 33(145\,pcf)^{1.5}\sqrt{4000\,psi} = 3644147\,psi \qquad (4\text{-}5)$$

Table 4-13: Selected Input Values for Example Westergaard Equation Calculations

Input Values for Westergaard Comparison	
Concrete Compressive Strength, f'_c (psi)	4000
Modulus of Elasticity of Concrete, E_c (psi)	3644147
Poisson's Ratio, ν	0.15
Load, P (lb)	21600
Modulus of Rupture, f_r (psi)	474
Radius of Circular Loading Area, a (in)	5.73

Table 4-14: Westergaard Stress Equation Calculation Results

Slab Thickness, *t* (in)	**Subgrade Modulus, *k* (pci)**	**Radius of Relative Stiffness, *l* (in)**	**Stress in Slab (psi) for Each Loading Condition**		
			Corner-Loading	*Interior-Loading*	*Edge-Loading*
6	50	34.0	1039	611	861
	100	28.6	956	554	758
	150	25.9	903	520	697
	200	24.1	863	497	654
7	50	38.2	801	460	653
	100	32.1	744	418	577
	150	29.0	707	394	533
	200	27.0	680	376	501
8	50	42.2	636	358	511
	100	35.5	595	326	452
	150	32.1	569	307	418
	200	29.9	550	294	394
9	50	46.1	518	286	409
	100	38.8	487	261	363
	150	35.1	468	246	336
	200	32.6	453	235	317
10	50	49.9	430	233	334
	100	42.0	406	212	297
	150	37.9	391	200	275
	200	35.3	380	192	259
11	50	53.6	363	193	277
	100	45.1	344	176	246
	150	40.7	332	166	228
	200	37.9	323	159	216
12	50	57.2	311	163	233
	100	48.1	295	148	207
	150	43.5	286	140	192
	200	40.5	279	134	182

Several conclusions were made based on calculation results. First, as slab-on-ground thickness increases, the stress in the slab decreases. This agrees with the relationships evident between thickness and stress in the PCA and UFC/COE design charts. Second, as the modulus of subgrade reaction increases, the stress in the slab decreases. Again, this relationship is evident in the PCA and UFC/COE design charts. Finally, the stress in the slab is highest under the corner loading condition and lowest under the interior loading condition. This finding was confirmed by agreement with results published for Murphy's 1937 computations of the stresses in loaded rectangular plates on elastic solids. Murphy found that the edge loading condition produces higher stresses than the interior loading condition (Murphy, 1937). Furthermore, Murphy also found that an increase in the subgrade modulus resulted in a reduction of the stresses in the slab-on-ground.

CHAPTER 5: CONCLUSIONS OF RESEARCH

5.1 RESEARCH ACHIEVEMENTS

This research has successfully provided a historical timeline review of each important step in the evolution of the design process of slabs-on-ground. This timeline included equations for the stress and deflections of a concrete slab-on-ground provided by various researchers throughout history, most notably those theorized by Harold M. Westergaard.

A review and analysis into the origins of the Portland Cement Association, Unified Facilities Criteria, Corps of Engineers, and American Concrete Institute methods for the selection of slab-on-ground design thickness revealed that each method is based on Westergaard's stress equations to various degrees. Specifically, it was determined that the Portland Cement Association method was based on the influence charts designed by Pickett and

Ray in the 1950s which are based on a modified version of Westergaard's equations. In addition, the design chart used in the PCA method, in Chapter 2, was found to be only applicable in interior loading conditions. The design chart created by the Corps of Engineers and used in the Unified Facilities Criteria guide for slabs-on-ground subjected to heavy loads was determined to be only applicable in edge loading conditions.

Research results showed good agreement between the slab-on-ground design thickness results using the Portland Cement Association method and the American Concrete Institute method for unreinforced slabs-on-ground subject to an interior loading condition. The Portland Cement Association (1955) explicitly states that a factor of safety is not built into the design chart.

Results for slab thickness using the Unified Facilities Criteria and Corps of Engineers design chart method were slightly lower than the resulting slab thickness using the ACI method for unreinforced slabs-on-ground subject to an edge loading condition. This research concluded that the ACI 360 manual (2010) asserts that the chart appearing in the COE and UFC methods is based on the following built-in provisions: using an impact factor of 25%, a concrete modulus of elasticity of 4000 kips per square inch, and a factor of safety of 2. Because it is not clear what role each of these play within the design chart, it was determined that the factor of safety in the UFC/COE design chart is somehow included in the form of a severity rating or design index rather than just a specific multiplier built into the chart. Within the UFC 3-320-06A design guide, there is no information that provides an explanation of factors of safety involved in the use of the design chart nor its origins. The only evident safety provision was the use of the design index and the assumption of the flexural strength of the concrete to be equal to the modulus of rupture. Therefore, it was concluded that a factor of safety is built into the design

chart in the form of a severity rating called the design index. The design index serves as a safety provision in addition to limiting the maximum stress to a value equal to the modulus of rupture of the concrete.

5.2 SUGGESTIONS FOR FUTURE WORK

The original equations of Harold M. Westergaard are well-documented, however the governing differential equations and computations Westergaard used to develop his edge, corner, and interior loading condition equations are unknown. This is due to two reasons: firstly, his work was originally written in Danish and not all of it has been translated to English; secondly, the work was not documented or was lost over the years. Ever-evolving technology may have interfered with the preservation of his work or the lack of digital file storage during Westergaard's time may have contributed to this loss. It is also possible that Westergaard chose not to publish his governing differential equations and calculations and to simply publish the resulting equations. The disagreement in results between results for the Corp of Engineers method and the ACI 360 edge-loading results also raised concern. Further research into this issue would be greatly beneficial in defining the foundational mathematics involved in the design of slabs-on-ground. In addition, further investigation into the creation of the Corps of Engineers design chart for slab thickness selection may clarify the built-in factors of safety identified by this research.

REFERENCES

ACI Committee 302. 2004. *ACI 302.1R-04: Guide for Concrete Floor and Slab Construction*. American Concrete Institute.

ACI Committee 302. *ACI 302.2R: Guide for Concrete Slabs that Receive Moisture-Sensitive Flooring Materials.* American Concrete Institute.

ACI Committee 360. 2010. *ACI 360R-10: Guide to Design of Slabs-on-Ground*. American Concrete Institute.

ACI Committee 544. *ACI 544: Fiber Reinforced Concrete.* American Concrete Institute.

Barnett, Robert. *Misawa Block 50 F-16 Upgrades*. 2008. Photograph. *Air Force Medical Service*. United States Air Force. https://www.airforcemedicine.af.mil/MTF/Misawa/News-Events/Article/403922/misawa-f-16s-undergo-upgrade-program/. Accessed November 2018.

Boussinesq, V. Joseph, "Application des potentiels a l'étude de l'équilibre et du mouvement des solides élastiques, avec des notes étendues sur divers points de physique mathématique et d'analyse", (Application of Potential to the Study of the Equilibrium and Movement of Elastic Solids, Particularly the Calculation of Deformations and Stresses Produced Within Such Solids, by Some Load Applied Upon a Small Portion of Their Surface or Their Interior: Continuous Paper from Extensive Notes on Diverse Points of Physical Mathematics and Analysis). Gauthier-Villars, Paris, 1885.

Brink, Anna Catharina. *Modelling Aggregate Interlock Load Transfer at Concrete Pavement Joints*. Master's thesis, University of Pretoria, 2003.

Delatte, Norbert. 2008. *Concrete Pavement Design, Construction, and Performance*. New York, NY: Taylor & Francis.

Dey, Arindam, Prabir Kumar Basudhar, and Sarvesh Chandra. 2011. "Distribution of Subgrade Modulus beneath Beams on Reinforced Elastic Foundations." *Indian Geotechnical Journal* 42 (2): 54–63.

Dinan, Robert. UFC 3-320-06A: Heavily Loaded Floor Slab Design Revision Meeting Notes (Microsoft Excel). May 13, 2016.

Donnally, Vincent R. 2016. "Hangar Pavement Design." Optimize Energy Use | WBDG Whole Building Design Guide. December 9, 2016. https://www.wbdg.org/resources/hangar-pavement-design. Accessed November 27, 2017.

Eberhardt, A. C. 1973. “Analysis of Pickett’s Solution to Westergaard’s Equation for Rigid Pavements”. Department of the Army. Construction Engineering Research Laboratory.

Eftis, J., and H. Liebowitz. 1972. “On the Modified Westergaard Equations for Certain Plane Crack Problems.” *International Journal of Fracture Mechanics* 8 (4): 383–92. https://doi.org/10.1007/bf00191100.

Engineering ToolBox. 2003. *Equivalent Diameter*. [online] Available at: https://www.engineeringtoolbox.com/equivalent-diameter-d_205.html [Accessed 13 Nov. 2018].

“F-16 Fighting Falcon.” n.d. Lockheed Martin. Accessed November 13, 2018. https://www.lockheedmartin.com/en-us/products/f-16.html.

Feldmann, Terry, PE, and Alan Schambach, PE. "Design of Slabs on Grade." *Frame Building News*, January 2016, 1-4. Accessed September 24, 2018. http://www.constructionmagnet.com/frame-building-news.

Frýba, Ladislav. 1995. History of Winkler Foundation, Vehicle System Dynamics, 24:sup1, 7-12, DOI: 10.1080/00423119508969611

Goldbeck, A. T., “Thickness of Concrete Slabs,” *Public Roads*, Vol. 1, No. 12, April, 1919.

Huang, Yang H. *Pavement Analysis and Design*. Englewood Cliffs, NJ: Prentice Hall, 1996.

Ioannides, Anastasios Michael, M.I. Hammons. “A Westergaard-Type Solution for the Edge Load Transfer Problem.” *Transportation Research Record: Journal of the Transportation Research Board*, no. 1525 (1996). Accessed November 2018. https://doi.org/10.3141/1525-04

Ioannides, Anastasios Michael, M. R. Thompson, and E. J. Barenberg. "Westergaard Solutions Reconsidered." *Transportation Research Record: Journal of the Transportation Research Board*, no. 1043 (1985): 13-23. Accessed September 2017. http://onlinepubs.trb.org/Onlinepubs/trr/1985/1043/1043-003.pdf.

Ioannides, Anastasios Michael, M. R. Thompson, J. Donnelly, and E. J. Barenberg. *Analysis of Slabs-on-grade for a Variety of Loading and Support Conditions*. PhD diss., University of Illinois at Urbana-Champaign, 1984.

Krishna Rao, K. V., PhD. "Stresses in Rigid Pavements." Lecture. Accessed September 19, 2018. https://www.civil.iitb.ac.in/~kvkrao/index.html.

Lstiburek, Joseph W. "Concrete Floor Problems." *Insight*, no. 003 (May 2008): 1-6. Accessed January 2018.

Lstiburek, Joseph W. "Slab Happy." *Insight*, no. 059 (August 2012): 1-6. Accessed January 2018.

MacGregor, C. W., The Potential Function Method for The Solution of Two-Dimensional Stress Problems, *Trans. Am. Math. Soc*., 38 (1935).

McKinney, Arthur W. 2007. "ACI 360R-06 Brings Slabs on Ground Design into the 21st Century." *Structure*, January 2007.

Mellgren. 1980. Ecoefficient Timber Forwarding on Lowland Soft Soils - Scientific Figure on ResearchGate. Available from: https://www.researchgate.net/Calculation-of-Nominal-Ground-Pressure_fig3_224830979 [accessed 12 Nov, 2018]

Michelin. 2015. *Michelin Military Aircraft Tires*. Accessed November 12, 2018. https://aircraft.michelin.com/wp-content/uploads/2017/12/2015_Military_Brochure.pdf.

Murphy, G., 1937. Stresses and deflections in loaded rectangular plates on elastic foundations. Bulletin No. 135 Iowa State College of Agriculture and Mechanic Arts.

Older, C., "Highway Research in Illinois," Transactions, ASCE, Vol. 87, 1927.

Pickett, G., "Concrete Pavement Design: Appendix III – A Study of Stresses in the Corner Region of Concrete Pavement Slabs Under Large Corner Loads," Portland Cement Association, 1946.

Pickett, G., Raville, M.E., Janes, W.C. and McCormick, F.J., 1951. "Deflections, moments and reactive pressures for concrete pavements", Bulletin No. 65. Engineering Experiment Station.

Pickett, G., Ray, G. K., "Influence Charts for Concrete Pavements," Transactions, ASCE, Vol. 116, 1951, p. 49.

Portland Cement Association, The. 1955. *Design of Concrete Airport Pavements*. Chicago, Illinois.

Rice, J. L., A. C. Eberhardt, and L. Varga. *Development of a Design Manual for Concrete Floor Slabs on Grade*. Army Construction Engineering Research Laboratory. January 1974.

Ringo, Boyd C., 1986, "Design Workshop for Industrial Slabs-on-Ground," *Seminar Booklet, World of Concrete*, Concrete Construction Publications, Addison, IL.

Ringo, Boyd C., and Robert B. Anderson. *Designing Floor Slabs on Grade: Step-by-step Procedures, Sample Solutions, and Commentary*. Second ed. Addison, IL: Aberdeen Group, 1996.

Ringo, Boyd C., and Robert B. Anderson. "Choosing Design Methods for Industrial Floor Slabs." *Concrete Construction*, April 1, 1994. Accessed July 10, 2018. https://www.concreteconstruction.net/how-to/choosing-design-methods-for-industrial-floor-slabs_o.

Tabatabaie, A.M., Barenberg, E.J., and Smith, R.E., "Longitudinal Joint Systems in Slip-Formed Rigid Pavements, Volume II – Analysis of Load Transfer Systems for Concrete Pavements," U.S. Department of Transportation, Report No. FAA-RD-79-4, II, November, 1979.

U. S. Department of Defense. *Pavement Design For Airfields*. Unified Facilities Criteria 3-260-02. 2001.

U. S. Department of Defense. *Concrete Crack and Partial-Depth Spall Repair*. Unified Facilities Criteria 3-270-03. 2001.

U. S. Department of Defense. *Concrete Floor Slabs on Grade Subjected to Heavy Loads*. Unified Facilities Criteria 3-320-06A. 2005.

U. S. Department of Defense. *Pavement Design For Airfields*. Unified Facilities Criteria 3-260-06. 2001.

U. S. Department of Defense. *Aircraft Maintenance Hangars: Type I, Type II and Type III*. Unified Facilities Criteria 4-211-01N. 2004.

U. S. Departments of the Army and the Air Force. *Concrete Floor Slabs on Grade Subjected to Heavy Loads*. Army TM 5-809-12. Air Force AFM 88-3, Chap. 15. August 1987.

Valdebenito, M. A., C. A. Pérez, H. A. Jensen, and M. Beer. "Approximate Fuzzy Analysis of Linear Structural Systems Applying Intervening Variables." *Computers & Structures* 162 (January 1, 2016): 116-29. Accessed January 31, 2018. doi:10.1016/j.compstruc.2015.08.020.

Westergaard, Harold M. "Om Beregning af Plader paa elastik Underlag med saerlight Henblik paa Sporgsmaalet om Paendinger i Betonveje," (On the Design of Plates on Elastic Foundation with Special Reference to Stresses in Concrete Pavements), *Ingenioren*, Vol. 32, Copenhagen, 1923.

Westergaard, Harold M. "Theory of Stresses in Road Slabs." In *Proceedings of the Fourth Annual Meeting of the Highway Research Board*, 60-61. National Research Council Building, Washington, D.C. Vol. 4. Highway Research Board, 1924.

Westergaard, Harold M. "Computation of Stresses in Concrete Roads." In *Proceedings of the Fifth Annual Meeting of the Highway Research Board*, 90-113. Washington, D.C. Vol. 5. 1925.

Westergaard, Harold M. "Stresses in Concrete Pavements Computed by Theoretical Analysis." *Public Roads* Vol. 7, no. 1 (March 1926): 25-35.

Westergaard, Harold M. "Analysis of Stresses in Concrete Roads Caused by Variations of Temperature." *Public Roads* Vol. 8, no. 3 (May 1927): 54-60.

Westergaard, Harold M. “Analytical Tools for Judging Results of Structural Tests of Concrete Pavements,” *Public Roads*, Vol. 14, no. 10 (December 1933).

Westergaard, Harold M. “What is Known of Stresses,” *Engineering News Record*, January, 1937.

Westergaard, Harold M. “Stresses in Concrete Runways of Airports,” Proceedings, 19th Annual Meeting, Highway Research Board, Washington, D. C., 1939.

Westergaard, Harold M. “Stress Concentrations in Plates Loaded over Small Areas,” ASCE Transactions, Vol. 108, 1943.

Westergaard, Harold M. “New Formulas for Stresses in Concrete Pavements of Airfields,” ASCE Proceedings, Vol. 73, No. 5, May, 1947.

Westergaard, Harold M. 1952. *Theory of Elasticity and Plasticity*. 3rd ed. Harvard Monographs in Applied Science. Cambridge, MA: Harvard & Wiley.

Winkler, Emil. *Die Lehre Von Der Elastizität Und Festigkeit*. Dominicius, 1868.